# Radiocesium transfer from hillslopes to the Pacific Ocean after the Fukushima Nuclear Power Plant accident: A review

O. Evrard, Jean-Patrick Laceby, Hugo Lepage, Yuichi Onda, Olivier Cerdan,
Sophie Ayrault

# Radiocesium transfer from hillslopes to the Pacific Ocean after the Fukushima Nuclear Power Plant accident: A review

**Olivier Evrard**[a], **J. Patrick Laceby**[a]**, Hugo Lepage**[a]**, Yuichi Onda**[b]**, Olivier Cerdan**[c]**, Sophie Ayrault**[a]

[a]Laboratoire des Sciences du Climat et de l'Environnement (LSCE), Unité Mixte de Recherche 8212 (CEA-CNRS-UVSQ/IPSL), Gif-sur-Yvette, France

[b]Graduate School of Life and Environmental Sciences, Center for Research in Isotopes and Environmental Dynamics (CRIED), University of Tsukuba, Tsukuba, Japan

[c]Bureau de Recherches Géologiques et Minières, Orléans, France

Corresponding Author: O. Evrard (Olivier.Evrard@lsce.ipsl.fr)

### Highlights

- The majority of radiocesium is transported in the particulate fraction.
- The contribution of the dissolved fraction is only relevant in base flows.
- Significant transfer of particulate-bound radiocesium occurs during heavy rainfall.
- Radiocesium deposited in floodplains may be remobilized, inducing contamination.
- Transdisciplinary approach is required to quantify radiocesium transfers.

1 **Radiocesium transfer from hillslopes to the Pacific Ocean after the Fukushima**

2 **Nuclear Power Plant accident: A review**

3

4 **Abstract:**

5 The devastating tsunami triggered by the Great East Japan Earthquake on March 11, 2011
6 inundated the Fukushima Dai-ichi Nuclear Power Plant (FDNPP) resulting in a loss of cooling
7 and a series of explosions releasing the largest quantity of radioactive material into the
8 atmosphere since the Chernobyl nuclear accident. Although 80% of the radionuclides from
9 this accidental release were transported over the Pacific Ocean, 20% were deposited over
10 Japanese coastal catchments that are subject to frequent typhoons. Among the
11 radioisotopes released during the FDNPP accident, radiocesium ($^{134}$Cs and $^{137}$Cs) is
12 considered the most serious current and future health risk for the local population.

13 The goal of this review is to synthesize research relevant to the transfer of FDNPP derived
14 radiocesium from hillslopes to the Pacific Ocean. After radiocesium fallout deposition on
15 vegetation and soils, the contamination may remain stored in forest canopies, in vegetative
16 litter on the ground, or in the soil. Once radiocesium contacts soil, it is quickly and almost
17 irreversibly bound to fine soil particles. The kinetic energy of raindrops instigates the
18 displacement of soil particles, and their bound radiocesium, which may be mobilized and
19 transported with overland flow. Soil erosion is one of the main processes transferring
20 particle-bound radiocesium from hillslopes through rivers and streams, and ultimately to the
21 Pacific Ocean. Accordingly this review will summarize results regarding the fundamental
22 processes and dynamics that govern radiocesium transfer from hillslopes to the Pacific
23 Ocean published in the literature within the first four years after the FDNPP accident.

24 The majority of radiocesium is reported to be transported in the particulate fraction and is
25 attached to fine particle size fractions. The contribution of the dissolved fraction to
26 radiocesium migration is only relevant in base flows and is hypothesized to decline over
27 time. Owing to the hydro-meteorological context of the Fukushima region, the most
28 significant transfer of particulate-bound radiocesium occurs during major rainfall and runoff
29 events (e.g. typhoons and spring snowmelt). There may be radiocesium storage within
30 catchments in forests, floodplains and even within hillslopes that may be remobilized and
31 contaminate downstream areas, even areas that did not receive fallout or may have been
32 decontaminated.

33 Overall this review demonstrates that characterizing the different mechanisms and factors
34 driving radiocesium transfer is important. In particular, the review determined that
35 quantifying the remaining catchment radiocesium inventory allows for a relative comparison
36 of radiocesium transfer research from hillslope to catchment scales. Further, owing to the
37 variety of mechanisms and factors, a transdisciplinary approach is required involving
38 geomorphologists, hydrologists, soil and forestry scientists, and mathematical modellers to
39 comprehensively quantify radiocesium transfers and dynamics. Characterizing radiocesium
40 transfers from hillslopes to the Pacific Ocean is necessary for ongoing decontamination and
41 management interventions with the objective of reducing the gamma radiation exposure to
42 the local population.

43     **Key Words (Max 6):** Fukushima, Cesium, Soil, Sediment, Forest, Modelling

44

45     **Graphical Abstract:**



46
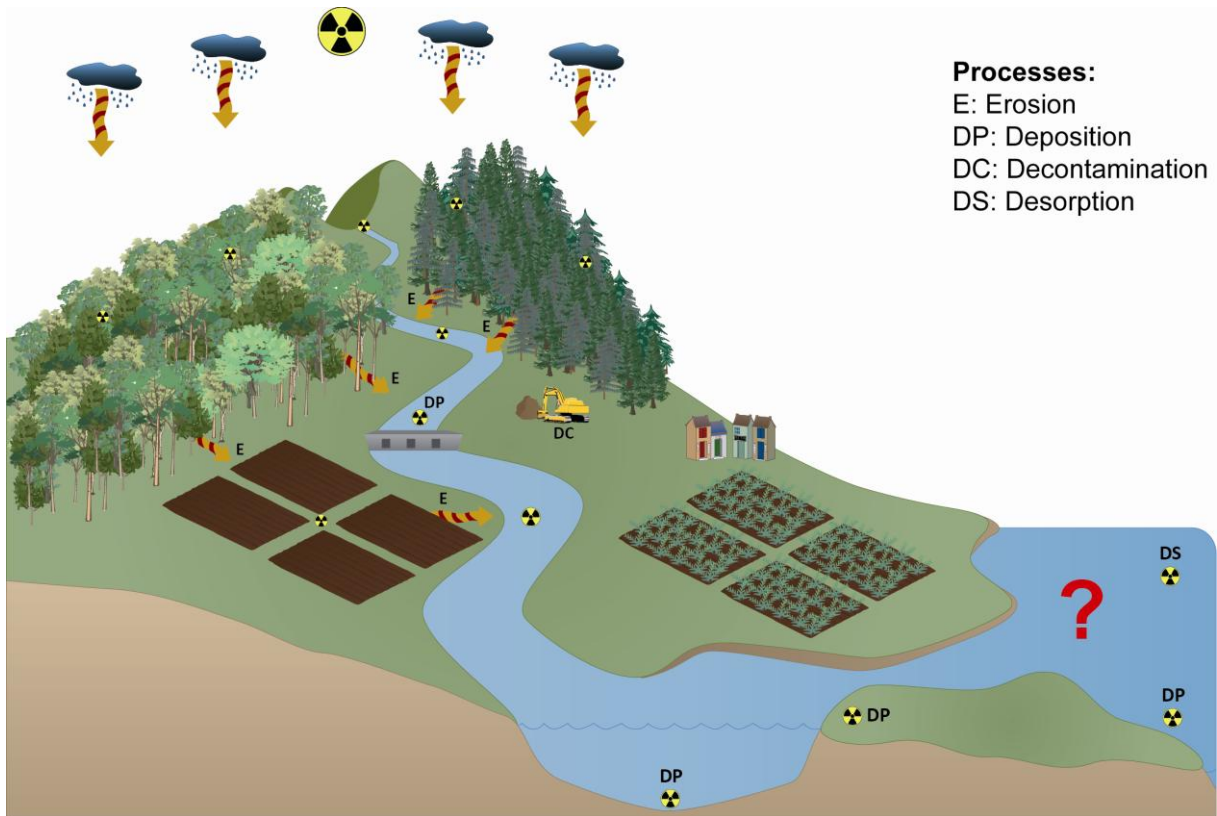
**Introduction**

48    The Great East Japan Earthquake on March 11, 2011 generated a giant tsunami inundating the

49    Fukushima Dai-ichi Nuclear Power Plant (FDNPP). After the loss of cooling at three FDNPP reactors, a

50    series of explosions occurred resulting in a massive release of radioactive contaminants into the

51    atmosphere. The FDNPP accident resulted in the largest atmospheric release of radioactive material

52    since Chernobyl (Chino et al., 2011; Steinhauser, 2014; Thakur et al., 2013). Although 80% of the

53    fallout from this atmospheric release was over the ocean, 20% of fallout was over terrestrial Japan

54    (Groëll et al., 2014; Kawamura et al., 2011; Kobayashi et al., 2013). The terrestrial fallout from the

55    FDNPP accident occurred in a different environmental context than previous major accidents,

56    occurring predominantly in a coastal mountainous region subject to frequent typhoons (Hilton et al.,

57    2008; Shinomiya et al., 2014).

58    Radiocesium ($^{134}$Cs and $^{137}$Cs) is considered the most serious risk to the current and long term health

59    of the local population (Kitamura et al., 2014; Saito et al., 2015). The half-life of the two most

60    abundant radiocesium isotopes is 2 y ($^{134}$Cs) and 30 y ($^{137}$Cs). Therefore, FDNPP derived radiocesium

61    will be an ongoing, long-term source of gamma radiation exposure to the local population.

62    Accordingly, this review will focus on radiocesium transfer from hillslopes to the Pacific Ocean.

63    Shortly after the FDNPP accident, multiple other radioisotopes were measured in the environment.

64    The wet deposition of hazardous iodine ($^{131}$I, half-life of 8 d) was detected along with multiple short-

65    lived radionuclides (Shozugawa et al., 2012; Tagami et al., 2011; Tazoe et al., 2012) (Table 1).

66    However, these short-lived isotopes disappeared quickly and were primarily below detection limits

67    by late April 2011 (Fujiwara et al., 2012). Long-lived isotopes (e.g., $^{239}$Pu ($T_{1/2}$ = 24100 y), $^{240}$Pu ($T_{1/2}$ =

68    6560 y)) were also detected (Table 1), although only in trace levels (Evrard et al., 2014b; Schneider et

69    al., 2013; Schwantes et al., 2012). Steinhauser (2014) comprehensively reviewed radionuclides that

70    may have been released by the FDNPP accident which have received less attention. These

71    radionuclides include less volatile elements ($^{89}$Sr, $^{90}$Sr, $^{103}$Ru, $^{106}$Ru), pure beta-emitters ($^{3}$H, $^{14}$C, $^{35}$S),

72    gaseous radionuclides ($^{85}$Kr, $^{133}$Xe, $^{135}$Xe) or radionuclides with very long half-lives (e.g., $^{36}$Cl, $^{99}$Tc, $^{129}$I,

73    $^{236}$U)(Table 1).

**Table 1.** Radionuclides detected in environmental samples after the FDNPP accident

| Radionuclide | Half-life (d) | Half-life (y) | Reference |
|---|---|---|---|
| $^{129}$Te | 0.05 | -- | Tazoe et al. (2012) |
| $^{132}$I | 0.10 | -- | Shozugawa et al. (2012) |
| $^{135}$Xe | 0.38 | -- | Steinhauser (2014) |
| $^{91}$Sr | 0.40 | -- | Shozugawa et al. (2012) |
| $^{140}$La | 1.70 | -- | Shozugawa et al. (2012); Tagami et al. (2011) |
| $^{133m}$Xe | 2.20 | -- | Steinhauser (2014) |
| $^{239}$Np | 2.35 | -- | Shozugawa et al. (2012) |
| $^{132}$Te | 3.30 | -- | Shozugawa et al. (2012)) |
| $^{133}$Xe | 5.25 | -- | Steinhauser (2014) |
| $^{131}$I | 8.00 | -- | Shozugawa et al. (2012); Tagami et al. (2011); Tazoe et al. (2012) |
| $^{131m}$Xe | 11.90 | -- | Steinhauser (2014) |
| $^{140}$Ba | 12.80 | -- | Shozugawa et al. (2012) |
| $^{136}$Cs | 13.20 | -- | Tagami et al. (2011) |
| $^{129m}$Te | 33.60 | -- | Tagami et al. (2011); Tazoe et al. (2012) |
| $^{95}$Nb | 35.00 | -- | Shozugawa et al. (2012); Tagami et al. (2011) |
| $^{103}$Ru | 39.40 | -- | Steinhauser (2014) |
| $^{59}$Fe | 44.60 | -- | Shozugawa et al. (2012) |
| $^{89}$Sr | 50.53 | -- | Steinhauser (2014) |
| $^{91}$Y | 58.50 | -- | Shozugawa et al. (2012) |
| $^{95}$Zr | 64.00 | -- | Shozugawa et al. (2012) |
| $^{35}$S | 87.37 | -- | Steinhauser (2014) |
| $^{110m}$Ag | 252.00 | -- | Shozugawa et al. (2012); Tagami et al. (2011); Tazoe et al. (2012) |
| $^{134}$Cs | -- | 2.06 | Tagami et al. (2011); Tazoe et al. (2012) |
| $^{85}$Kr | -- | 10.75 | Steinhauser (2014) |
| $^{3}$H | -- | 12.32 | Kakiuchi et al. (2012); Steinhauser (2014) |
| $^{241}$Pu | -- | 14.33 | Steinhauser (2014) |
| $^{137}$Cs | -- | 30.20 | Shozugawa et al. (2012); Tagami et al. (2011); Tazoe et al. (2012) |
| $^{238}$Pu | -- | 87.70 | Steinhauser (2014) |
| $^{241}$Am | -- | 432.60 | Steinhauser (2014) |
| $^{14}$C | -- | 5730.00 | Steinhauser (2014) |
| $^{240}$Pu | -- | 6561.00 | Steinhauser (2014) |
| $^{239}$Pu | -- | 24110.00 | Shozugawa et al. (2012); Steinhauser (2014) |
| $^{99}$Tc | -- | 2.10E+05 | Steinhauser (2014) |
| $^{36}$Cl | -- | 3.00E+05 | Steinhauser (2014) |
| $^{129}$I | -- | 1.57E+07 | Steinhauser (2014) |
| $^{236}$U | -- | 2.34E+07 | Steinhauser (2014) |
| $^{235}$U | -- | 7.04E+08 | Steinhauser (2014) |
| $^{238}$U | -- | 4.47E+09 | Steinhauser (2014) |

74

75  Researching less abundant radionuclides may provide useful and complementary information on the

76  events that occurred at FDNPP (Achim et al., 2014; Le Petit et al., 2014). However, owing to the

77  potential gamma radiation exposure, there has been an increasing focus in the literature on the

78  transfer, fate, dynamics and consequences of radiocesium in the fallout impacted region. Before the

79  accident, there were on average six publications a year with Fukushima in the title (Fig. 1). After the

80  accident (from 2011 to 2014), this average increased over 50 fold to approximately 350 publications

81  a year. Of these publications, the percent of published research including radiocesium as a topic

82  increased from 8% in 2011 to 32% in 2014 indicating that radiocesium, in the fallout impacted region,

83  is of increasing significance to the scientific community.
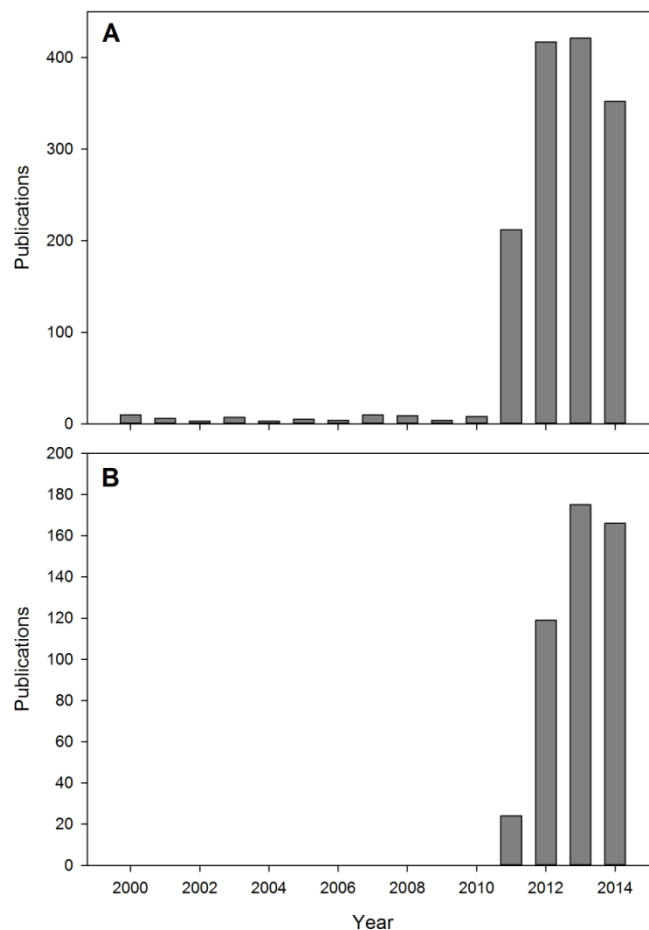


**Figure 1.** Annual publications with Fukushima in the title (A - top), and Fukushima in the title with Cesium/Caesium included the topic (B - bottom) from a Web of Science search conducted early in January 2015.

84

85　　Initially radiocesium was deposited on terrestrial vegetation and soils. Depending on local conditions,

86　　the contamination may remain stored in the forest canopy, in the vegetative litter on the ground or

87　　in the soil. Once radiocesium contacts soil, it is quickly and almost irreversibly bound to fine soil

88　　particles (He and Walling, 1996; Sawhiney, 1972; Tamura, 1964). During rainfall, the kinetic energy of

89　　raindrops instigates the displacement of soil particles and their bound radiocesium, which are

90　　mobilized and transported with rainfall runoff (Renard et al., 1991; Torri et al., 1987)(Fig. 2). Soil

91　　erosion is considered to be the main process transferring particle-bound radiocesium from hillslopes

92　　through rivers and streams, and ultimately to the Pacific Ocean (Yoshida and Kanda, 2012)(Fig. 2).

93
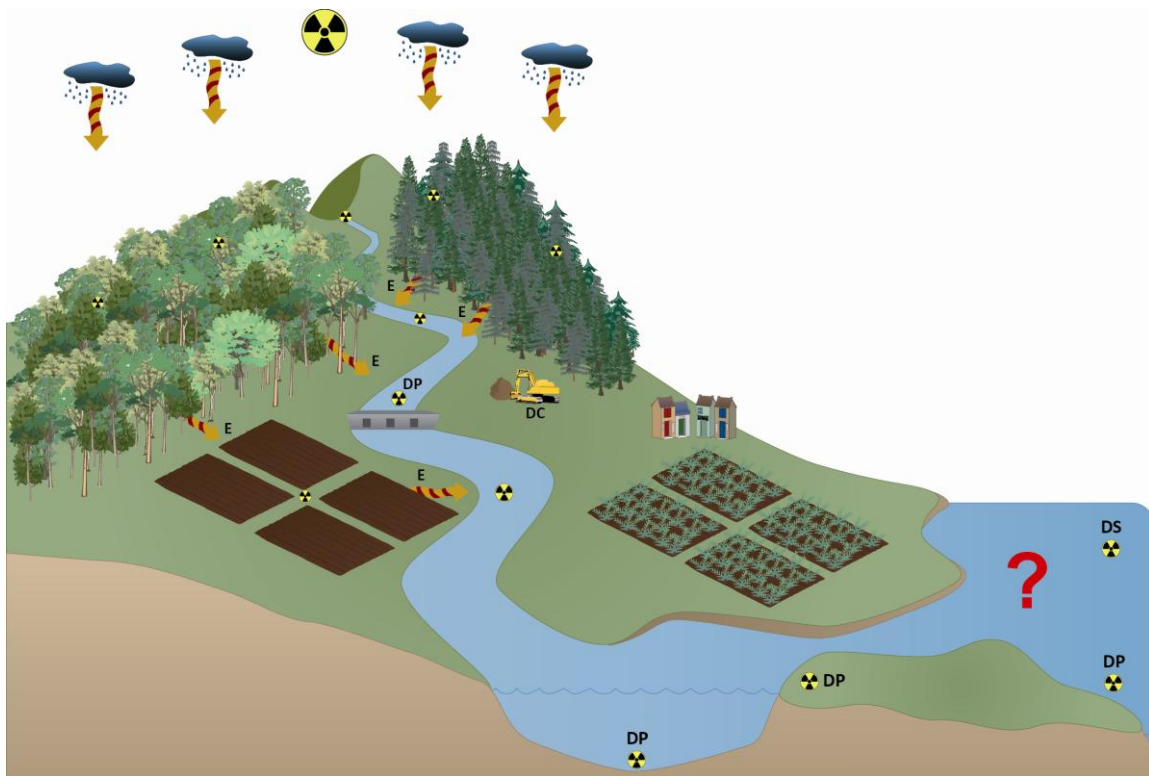
**Figure 2.** Potential pathways for radiocesium transfer from hillslopes to the Pacific Ocean following the FDNPP
accident denoting major processes such as erosion (E), deposition (DP), decontamination (DC) and desorption
(DS) (Images courtesy of the Integration and Application Network, University of Maryland Center for
Environmental Science (ian.umces.edu/symbols/)).

98

99　　The transfer of particulate-bound radiocesium may be substantial during typhoons typically occurring

100　　between June and October in Japan. Importantly, the fine particles, to which radiocesium is

101　　preferentially bound to, are the particles that are preferentially eroded and likely to be transported

102      the farthest during erosive rainfall events (Govers, 1985; Malam Issa et al., 2006; Motha et al., 2002).

103      Fundamentally, soil erosion and riverine transport processes are the primary factors governing the

104      long-distance transfer of radiocesium from hillslopes to the Pacific Ocean (Kitamura et al., 2015; Saito

105      and Onda, 2015; Yamada et al., 2015).

106      The goal of this review is to synthesize research relevant to the transfer of FDNPP derived

107      radiocesium outlined in the previous paragraph. The main objective is to comprehensively review

108      literature investigating the fundamental processes and dynamics governing radiocesium transfer

109      from hillslopes to the Pacific Ocean published within 4 y of the FDNPP accident. This review will

110      conclude with recommendations for future research and for the design and implementation of

111      effective countermeasures.

112      **1. Fallout radiocesium deposition**

113      Although radionuclides from the FDNPP accident were detected worldwide (Evrard et al., 2012; Long

114      et al., 2012; Masson et al., 2011; Wetherbee et al., 2012), the majority of terrestrial deposition

115      occurred in the Fukushima Prefecture. The main radiocesium plume is located northwest of the

116      FDNPP, with a secondary plume in the Abukuma River Valley southwest from Fukushima City past

117      Koriyama (Fig. 3). There are multiple approaches to quantify catchment radiocesium inventories

118      including both airborne and soil sampling surveys (Gonze et al., 2014; Saito et al., 2015; Yoshida and

119      Takahashi, 2012). As this review examines the transfer of radiocesium from hillslopes to the Pacific

120      Ocean, we used soil sampling surveys to quantify the total, mean, and standard deviation of

121      radiocesium ($^{134}$Cs+$^{137}$Cs) fallout in 14 coastal catchments of the Fukushima region (Fig. 3, Table 2).

122      This quantification of catchment inventories is based on the spatial interpretation conducted by

123      Chartin et al. (2013) of 2200 soil samples collected by the Japanese Ministry of Education, Culture,

124      Sports, Science and Technology (MEXT, 2012) between June and July 2011.

125
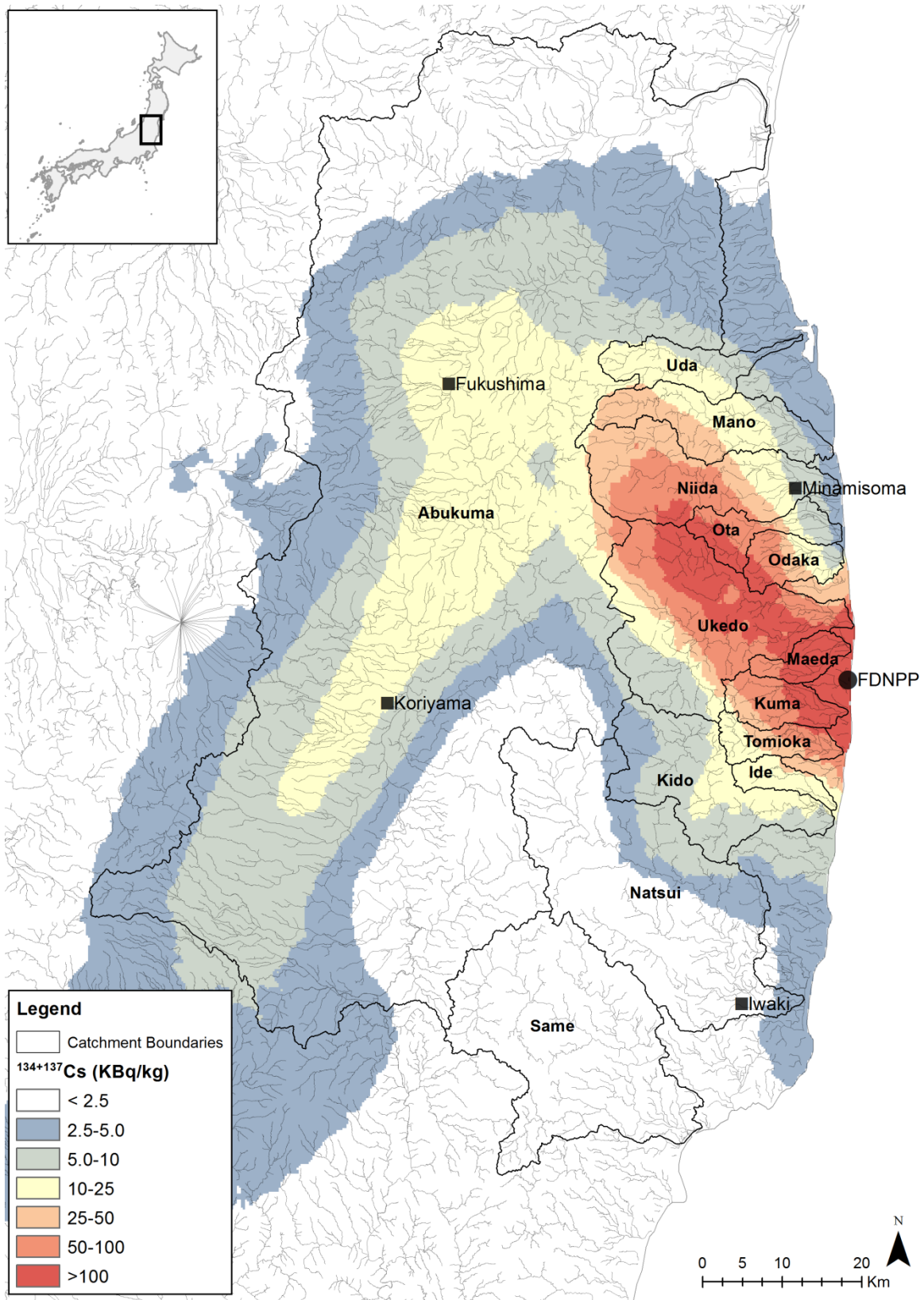
**Figure 3.** Labelled coastal catchments impacted by the fallout from the FDNPP accident, major rivers (grey lines), the location of the FDNPP (black circle) and major cities (black squares), and the spatial distribution of radiocesium fallout ($^{134}$Cs + $^{137}$Cs) in kBq/kg provided by Chartin et al. (2013) who spatially interpreted (ordinary kriging) the radiocesium distribution of 2200 soil samples taken by the Japanese Ministry of Education, Culture, Sports, Science and Technology (MEXT) between June and July 2011 decay corrected to June 14, 2011.

**Table 2.** Radiocesium ($^{134}$Cs+$^{137}$Cs) inventory received by the major coastal catchments in Fukushima region (Coastal catchment data derived from the Japanese Ministry of Land, Infrastructure, Transport and Tourism (http://nlftp.mlit.go.jp/ksj-e/index.html)) and the radiocesium inventories were calculated with data from Chartin et al. (2013) spatially interpreted radiocesium inventory calculations from Fig. 3 converted to total Cs from Bg/kg.

| Catchment | Area (km$^2$) | Total Inventory (TBq) | % of Total Inventory | Deposition Density (TBq km$^{-2}$) |
|---|---|---|---|---|
| Abukuma | 5338 | 734.9 | 30% | 0.14 |
| Ukedo | 423 | 643.9 | 26% | 1.52 |
| Niida | 265 | 283.4 | 12% | 1.07 |
| Kuma | 75 | 161.4 | 7% | 2.14 |
| Maeda | 45 | 149.9 | 6% | 3.32 |
| Ota | 77 | 111.0 | 5% | 1.44 |
| Odaka | 68 | 81.4 | 3% | 1.20 |
| Mano | 171 | 78.1 | 3% | 0.46 |
| Tomioka | 62 | 58.6 | 2% | 0.95 |
| Kido | 263 | 48.6 | 2% | 0.18 |
| Natsui | 696 | 36.3 | 1% | 0.05 |
| Uda | 101 | 27.6 | 1% | 0.27 |
| Same | 601 | 19.2 | 1% | 0.03 |
| Ide | 40 | 16.2 | 1% | 0.14 |

126

127 The Abukuma catchment received the most radiocesium fallout, followed by the Ukedo and Niida

128 catchments (Table 2). Radiocesium inventories for the 14 coastal catchments ranged between 734.9

129 TBq in the Abukuma to 16.2 TBq in the Ide catchment. The Abukuma catchment received

130 approximately 30% of the fallout received by these 14 catchments, followed by 26% for the Ukedo

131 and 12% for the Niida. Although the Abukuma catchment received the highest amount of fallout, the

132 radiocesium was distributed over a broad spatial area and the mean deposition density in the

133 Abukuma catchment was 0.14 TBq km$^2$. Comparatively, the smaller coastal catchments had the

134 highest mean radiocesium inventories, particularly the Meada (3.32 TBq km$^{-2}$), Kuma (2.14 TBq km$^{-2}$),

135 Ukedo (1.52 TBq km$^{-2}$), Ota (1.44 TBq km$^{-2}$), Odaka (1.20 TBq km$^{-2}$), and Niida (1.07 TBq km$^{-2}$)

136 catchments.

137 Although quantifying catchment inventories with airborne and soil based sampling techniques or

138 different spatial interpretation approaches may yield different results (Gonze et al., 2014), what is

9

139 important to the research and management community is the spatial distribution of radiocesium. In

140 particular, characterizing the deposition of radiocesium, especially the different catchments and

141 landscapes receiving the fallout (e.g different forest types), is important for understanding the

142 sources and spatial distribution of radiocesium available for transfer from hillslopes to the Pacific

143 Ocean.

### 2.1 Forest deposition

145 Significant radiocesium deposition occurred on forested landscapes. Approximately 66% of high

146 levels of radioactive fallout (> 1000 kBq.m$^{-2}$) took place over a mixture of deciduous and coniferous

147 forests (Hashimoto et al., 2012). As the accident occurred during late winter and deciduous trees had

148 no leaves, the fallout more directly contaminated the ground surface (soil and litter). In coniferous

149 forests, with their needles intact, the fallout radiocesium was partly intercepted by the forest

150 canopy. In particular, Kato et al. (2012a) estimated that between 62% and 65% of $^{137}$Cs was

151 intercepted by the canopies of cypress and cedar forests, respectively. When examining both

152 deciduous and coniferous forests, Koizumi et al. (2013) modelled that ~10% of the $^{137}$Cs deposited on

153 forests within the exclusion zone was trapped by biomass.

154 The majority of research has focused on Japanese Cedar (*Cryptomeria japonica*) followed by the mixed

155 forests and coniferous forest with broad leaf forests receiving the least attention (Fig. 4). The

156 research, in particular research examining Japanese Cedar, has been widespread throughout the

157 fallout impacted region and across northern Japan (Fig. 4). As the forested areas within 20 km of the

158 FDNPP (Koizumi et al., 2013) are approximately 50% broadleaf and 50% needle-leaf forest, it may be

159 advantageous for future research to examine radiocesium dynamics equally in broadleaf, coniferous

160 and mixed forests within the highly contaminated coastal catchments.

161 After canopy interception, the radiocesium transfer pathway from the canopy to the soil is complex

162 (Fig. 5). Radiocesium may transfer through leaf surface tissues or remain on the foliar surface. A

163 portion of foliar radiocesium (17 – 59%) was measured inside leaves within a year, whereas the

164 remaining radiocesium adhered to the leaf surface may be removed with wash off over time

165 (Koizumi et al., 2013; Nishikiori et al., 2015; Tanaka et al., 2013a). Results were similar for deciduous

166 (46% removed after washing) and coniferous canopies (41%) (Koizumi et al., 2013) indicative of a

167 potential long-term radiocesium source where canopies intercepted significant quantities of

168 radiocesium.
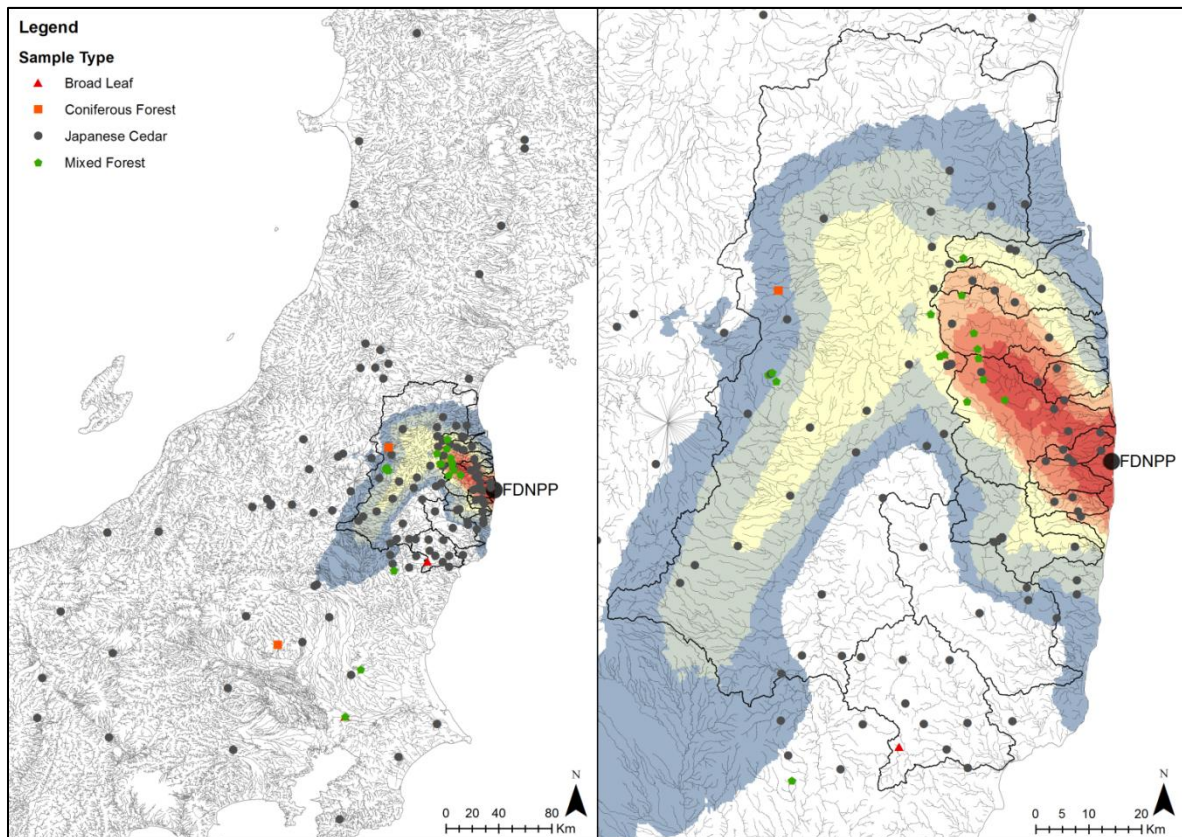


**Figure 4.** Localisation of samples examining radiocesium processes and dynamics in forests after the FDNPP Accident. Multiple samples may have been obtained at one location.

169 During the first year after the accident, foliar contamination was mainly due to the radiocesium

170 deposition. After the initial deposition, radiocesium may translocate between old and new vegetative

171 tissues (Nishikiori et al., 2015; Yoshihara et al., 2014b). In most studies, a decrease of contamination

172 was observed between old and young needles in coniferous forests (Akama et al., 2013; Kanasashi et

173 al., 2015; Nishikiori et al., 2015; Yoshihara et al., 2013). In contrast, Yoshihara et al. (2014b) reported

174 that new foliar growth in 2013 contained more radiocesium than 2011 samples in coniferous forests.

175 The variation between older and younger foliar components of coniferous forests contaminated by

176 the accident is complex and may impact the radiocesium export from these forests.

177
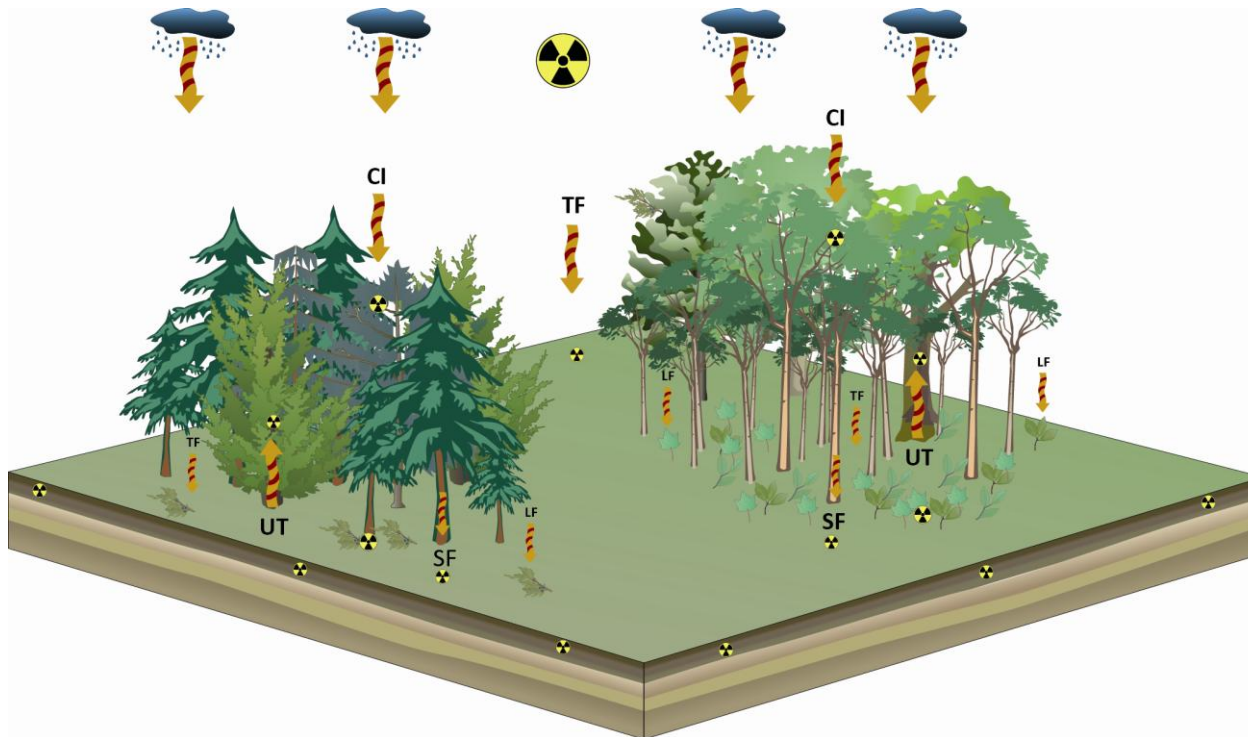


**Figure 5.** An illustration of the major radiocesium transfer pathways in forested (coniferous – to the left – and deciduous – to the right) landscapes. The major transfer pathways to the soil include throughfall (TF), canopy interception (CI), litter fall (LF) and stem flow (SF). There is also potential for the flora to uptake (UT) radiocesium (Images courtesy of the Integration and Application Network, University of Maryland Center for Environmental Science (ian.umces.edu/symbols/)).

178 For deciduous forests, research into foliar contamination is inconclusive. Tanaka et al. (2013a) did not

179 observe any contamination in new leaves. Nishikiori et al. (2015) reported that although leaves were

180 absent during the accident, contamination was detected in leaves sampled in 2012. Yoshihara et al.

181 (2014a) found no significant variation in leaves sampled in 2011 and 2012. Additional factors may

182 explain tree contamination such as root uptake, stem transfer, or surficial contamination due to

183 wind-eroded particle deposition.

184 Characterizing radiocesium transfer from forests to hillslopes is important for understanding

185 cumulative long-term radiocesium export from forest environments. During rainfall events,

186 radiocesium is more likely to be transferred by throughfall than by stemflow, although both

187     pathways increase ground contamination (Kato et al., 2012a; Loffredo et al., 2014). The effective

188     half-life of radiocesium in trees was calculated to be 620 d for cypress and 890 d for cedar canopies

189     (Kato et al., 2012a). Accordingly, there will likely be a medium to long-term canopy to ground

190     stemflow and throughfall transfer of radiocesium (Kato et al., 2012a).

191     Litterfall is a significant radiocesium transfer pathway. In fact, litterfall was reported to transfer as

192     much radiocesium as throughfall  (Teramage et al., 2014a). Further, Hasegawa et al. (2013) reported

193     that radiocesium concentrations in litter were greater than those measured in the soil. In the future,

194     litterfall will likely become the dominant pathway for radiocesium transfer from the canopy to the

195     forest floor as hydrological pathways transfer less radiocesium with time owing to decreased

196     availability (Teramage et al., 2014a). In addition, Kuroda et al. (2013) found that the tree bark was

197     highly contaminated. More than 94% of the stem contamination was located in the bark, indicative

198     of another potential long-term source of radiocesium derived either from surficial contamination or

199     through contaminated phloem sap.

200     The quantity of radiocesium in the litter depends on multiple factors such as tree species, location of

201     the forest in the radioactive pollution plume, or sampling date. Matsunaga et al. (2013) did not

202     observe specific migration of radiocesium from litter to soil after the first rainfall event (July-August

203     2011). Nakanishi et al. (2014) reported a decrease of $^{137}$Cs contamination in litter from 67% to 13%

204     during the first year, whereas contamination in soil increased from 26% to 80%. Takahashi et al.

205     (2015) found that the proportion of radiocesium in leaf litter, relative to soil, decreased from ~90% in

206     2011 to 18-14% in 2012. Fujii et al. (2014) also noted a significant decrease in the percentage of

207     radiocesium in the leaf litter, decreasing from between 44-65% in 2011 to 14-27% in 2012. The

208     transfer of radiocesium from litter to soil is controlled by rainfall and litter decomposition. Research

209     estimates that around 30%-40% of litter in Japanese forests is decomposed annually (Hashimoto et

210     al., 2012; Matsunaga et al., 2013).

211 In the Fukushima region, forests are a radiocesium reservoir, retaining significant quantities of

212 radiocesium within both the canopy and the leaf litter (Hashimoto et al., 2012; Koarashi et al.,

213 2012a). Although forested landscapes are not considered to be significant erosion sources

214 (Yoshimura et al., 2015a), there is an abundance of radiocesium within these systems, often stored in

215 organic matter, that may be transferred downstream during significant rainfall events. Accordingly,

216 forest landscapes may potentially become perennial sources of radiocesium in the Fukushima region.

217 Understanding both intra- and inter- forest radiocesium transfers will be fundamental to

218 understanding radiocesium transfer and export by soil erosion and wash-off. Incorporating

219 differences between deciduous and coniferous forests and their different rates of radiocesium

220 transfer is important for modelling hillslope exports and cumulative radiocesium transfers from

221 hillslopes to the Pacific Ocean.

222 *2.2 Soil deposition*

223 Upon contact with the soil, it is well known that radiocesium is strongly and rapidly fixated to fine soil

224 particles (He and Walling, 1996; Sawhiney, 1972). Cesium is an alkali metal and accordingly it

225 possesses similar chemical properties to potassium and may substitute for potassium in interactions

226 with clay minerals resulting in an almost irreversible fixation to fine soil particles (Kitamura et al.,

227 2015).

228 Following the Fukushima accident, researchers have extensively examined radiocesium fixation to

229 fine particles (Akai et al., 2013; Saito et al., 2014; Tanaka et al., 2013c). These examinations were

230 undertaken primarily because of the high organic matter and clay content of soils in the Fukushima

231 region that may influence the depth migration of radiocesium in the soil profile. In particular, there

232 has been a research focus on the physical and chemical foundation of the fixation of radiocesium to

233 fine particles and the depth migration of radiocesium in the soil profile. Characterizing the fixation

234 potential of radiocesium to fine soil particles is fundamental to understanding potential radiocesium

235   migration pathways including the mobilization and transport of radiocesium, and ultimately its

236   transfer through rivers and streams to the Pacific Ocean.

237   Compared to the forest radiocesium research, there has not been a similar regional coverage of soil

238   sampling across northern Japan (Fig. 6). The majority of samples examining soil transfer processes

239   including depth migration or fixation potential were taken within the 14 coastal catchments with a

240   well distributed coverage across the fallout impacted region. The focus of soil sampling is mainly on

241   paddy fields with a substantial number samples having unclassified land uses. The inclusion of land

242   use details would be beneficial to future research examining radiocesium transfer processes.
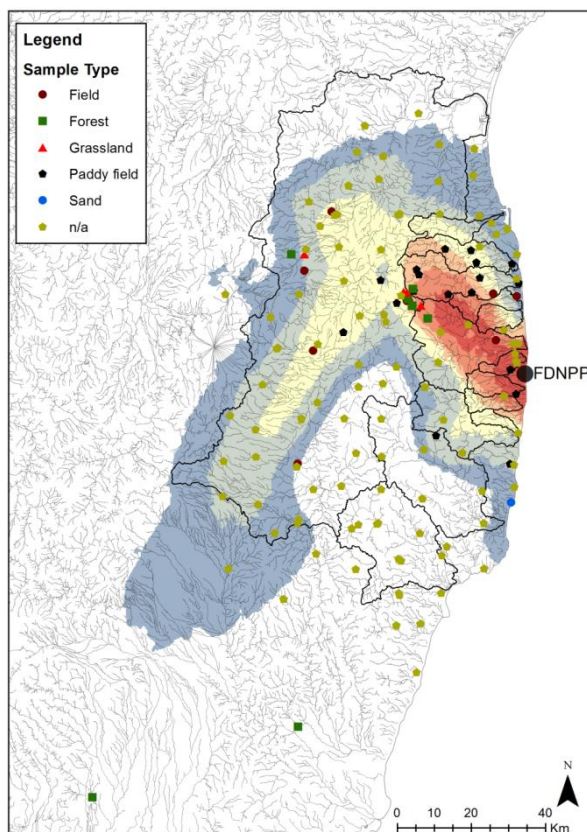


**Figure 6.** Location of soil sampling locations where research examined radiocesium dynamics or process such as depth migration in the soil profile or fixation to the mineral or soil fractions. More than one sample may occur at any given location.

243   Immediately after the FDNPP accident, Tanaka et al. (2013c) reported that the radiocesium was

244   water soluble, though once radiocesium adsorbed on to soil and rock particles it quickly became

245   essentially insoluble. The increase in insolubility was also reported by Shiozawa (2013) who indicated

246 that the strong fixation of radiocesium to clay particles during the initial 2–3 months after the

247 accident reduced the migration of radiocesium in the depth profile. The strong fixation to clay

248 particles was again reported by Saito et al. (2014) and Kikawada et al. (2014) who indicated that

249 virtually no radiocesium was extractable from soil samples with simple water solutions.

250 Using X-ray diffraction, Saito et al. (2014) reported that micaceous minerals (e.g. muscovite, biotite,

251 and illite) were responsible for the strong radiocesium soil fixation. Conversely, Kozai et al. (2012)

252 utilized desorption experiments to determine that radiocesium was almost irreversibly fixated to the

253 non-micaceous soil minerals. Niimura et al. (2015) reported that radiocesium fixation is due to a

254 physical adherence to the rough surfaces of the soil mineral particles. These different approaches to

255 understanding radiocesium fixation indicate that the physical processes behind this strong fixation

256 are difficult to characterize and are dependent upon multiple parameters such as experiment

257 characteristics, mineral contents, and/or the physical-chemical characteristics of both the fallout

258 radiocesium itself and the soil medium.

259 The extractability of radiocesium was found to be higher in forest soils with higher contents of clay

260 and silt particles, and a higher cation exchange capacity (Koarashi et al., 2012b). Using extraction

261 processes with $K_2SO_4$, Koarashi et al. (2012b) reported that only 2.1 to 12.8% of Fukushima-

262 originated radiocesium found in the surface mineral soils were retained as easily exchangeable ions

263 by abiotic components in forest sites. Potential uptake and retention of ^{137}Cs by microorganisms in

264 the forest surface soils (0-3 cm) were found to be minor and less important than ion-exchange

265 adsorption on non-specific sites provided by abiotic components (Koarashi et al., 2012b). In the long-

266 term, microorganisms in forest soils may contribute to the mobilization of radiocesium by

267 decomposition of the soil organic matter (e.g. leaf litter) (Koarashi et al., 2012b).

268 Research prior to the FDNPP accident clearly indicates that in undisturbed soils an exponential

269 decline of radiocesium in the soil profile is expected along with a very slow radiocesium depth

270 migration in the soil profile (He and Walling, 1997). In fact, the radiocesium peak from nuclear

271    weapons testing in the 1960s is now only 2-8 cm below the soil surface in undisturbed soils

272    (Jagercikova et al., 2015).

273    Owing to the strong and irreversible bond to fine soil particles, the majority of FDNPP derived

274    radiocesium currently remains stored within the top 5 cm of the soil profile in undisturbed soils

275    (Lepage et al., 2014b; Matsuda et al., 2015; Matsunaga et al., 2013; Mishra et al., 2015; Takahashi et

276    al., 2015). Anthropogenic activities increase the depth of migration of radiocesium in the soil profile

277    (Lepage et al., In Press; Matsunaga et al., 2013). Erosion and subsequent deposition processes may

278    also result in the increase of radiocesium with depth in the soil profile similarly to carbon and other

279    minerals in depositional landscapes (Van Oost et al., 2012). Lepage et al. (In Press) demonstrated that

280    90% of radiocesium remained in the upper 5 cm of the soil profile after deposition in non-cultivated

281    soils, whereas within cultivated soils the contamination was homogeneous throughout the tilled soil

282    layer (generally down to 15-30 cm). Endo et al. (2013) demonstrated that radiocesium

283    concentrations were not dependent on depth in rice paddy field soils, whereas they declined

284    exponentially in an uncultivated soil. Sakai et al. (2014) and Tanaka et al. (2013b) both indicated that

285    radiocesium from the FDNPP accident was measureable at 15 cm depth in rice paddy fields. Mishra

286    et al. (2015) reported that the vertical migration down the soil profile was slower in forest soils than

287    in grassland soils. In a study of 85 soil sampling sites, Matsuda et al. (2015) found that the depth

288    penetration of radiocesium was higher than the standard range (0.2-1.0 kg m$^{-2}$ y$^{-1}$) depicted by He

289    and Walling (1997).

290    Multiple researchers have postulated different hypotheses for the observed depth migration of

291    radiocesium in the soil profile. Fujiwara et al. (2012) reported that the elevated rates of radiocesium

292    migration down the soil profile are potentially indicative of the mobile form of radiocesium

293    immediately after the accident. Kato et al. (2012b) also observed increased downwards migration of

294    radiocesium immediately and attributed this phenomenon to high clay content that increased the

295    aggregate stability of topsoil resulting in increased water and radiocesium infiltration deeper into the

296    soil profile. Conversely, Satou et al. (2015) investigated the vertical migration in coarse-grained beach

297    material impacted by the tsunami. The authors demonstrated that the majority of radiocesium was

298    located at ~3-6 cm depth. This migration is likely due to coarser grained material indicative of a

299    potential particle size impact on the depth migration of radiocesium.

300    The depth migration of radiocesium also depends on soil properties. Koarashi et al. (2012a)

301    demonstrated that clay and organic matter content are key factors controlling radiocesium depth

302    migration. Organic matter inhibits the fixation of radiocesium on the soil mineral fraction by limiting

303    its access to adsorption sites on clay minerals through direct competition for potential adsorption

304    sites. As organic matter may limit the adsorption of radiocesium, it may also influence the rate of

305    radiocesium depth migration. The impact of organic matter is particularly notable in forests. The high

306    organic content of forest soils increases the potential for radiocesium depth migration (Koarashi et

307    al., 2012a). Nakanishi et al. (2014) demonstrated that 0.1% of the radiocesium deposited on the

308    forest floor indeed migrated below 10 cm depth in 1 y.

309    The timing and extent of rainfall may also drive the migration of radiocesium deeper within the soil

310    profile. The rainfall that occurred immediately after the accident fallout may have been a factor in

311    the radiocesium depth migration in forest soils (Teramage et al., 2014b) along with rainfall volume in

312    general (Fujii et al., 2014). Further, rainfall was listed as a potential factor for the depth migration in

313    the beach sand samples (Satou et al., 2015). The average rainfall in the Fukushima region is more

314    than 2 times greater than Chernobyl and the rainfall erosivity is almost 3 times greater (Laceby et al.,

315    submitted). Both the elevated rainfall intensity and volume may have resulted in greater depth

316    penetration of radiocesium in the Fukushima region compared to that of Chernobyl.

317    Migration of radiocesium was also correlated with low bulk densities as highly porous structures may

318    facilitate water and potentially dissolved radiocesium infiltration deeper down the soil profile

319    (Koarashi et al., 2012a; Takahashi et al., 2015). The radiocesium interception potential (RIP) is often

320    used to quantify this process. The RIP describes the capacity of the mineral content of soils to adsorb

321     radiocesium (Wauters et al., 1996). Fan et al. (2014b) reported the mean RIP from 13 soil samples

322     was 6.1 (with all discussed RIP values noted as mol.kg$^{-1}$). Nakao et al. (2014) noted a higher mean RIP

323     of 7.8 for 97 soil samples. Takahashi et al. (2015) reported a mean RIP of 4.1 for 7 soil samples and

324     demonstrated that RIP was negatively correlated with a penetration coefficient ($\alpha$), indicating that

325     the radiocesium penetrates deeper in soils with low RIP values. A similar relationship was found

326     between RIP values and the organic content of the soil with Takeda et al. (2014) confirming deeper

327     radiocesium penetration in soils with elevated organic content. In particular, Takeda et al. (2014)

328     reported a mean RIP for 46 samples of 2.4. Further, Koarashi et al. (2012a) reported a strong

329     negative correlation (r = -0.79, p < 0.005) between total organic carbon (TOC) content divided by clay

330     content (TOC/clay) and the percentage of retention of $^{137}$Cs, suggesting that the presence of organic

331     matter inhibits the adsorption of $^{137}$Cs on clay minerals.

332     Along with TOC, RIP depends on the presence of minerals having selective adsorption sites for Cs

333     (micas, micaceous clays) (Takeda et al., 2014). Indeed, the type of clay may be more important than

334     the total clay content as there were higher RIP values in soils containing clays from the micaceous,

335     vermiculitic and chloritic groups (>10 mol/kg)(Takahashi et al., 2015) than in soils containing clays of

336     amorphous and kaolinitic groups (Nakao et al., 2014). In the Fukushima region where some soils

337     developed on volcanic ash deposits, they contain higher amounts of poorly crystalline minerals (e.g.,

338     allophane, imogolite), which do not provide these adsorption sites (Takeda et al., 2014). There have

339     even been positive relationship between RIP and native K content which further reflects the fact that

340     the $^{137}$Cs retention ability of soil clays is controlled primarily by the amount of micaceous minerals

341     (Nakao et al., 2014). Ultimately, owing to the variety of relationships between TOC, clay content and

342     clay species, quantifying the dominant factors influencing RIP in the Fukushima region is more

343     complicated than in the Chernobyl region.

344     The research on radiocesium deposition on soils has focussed on understanding post-deposition

345     dynamics. In particular, understanding the RIP and concomitant fixation to soil is important to

346  understand post-deposition processes with important ramifications for management. For example,

347  owing to the strong fixation potential to soils, radiocesium will be maintained in the upper sections

348  of undisturbed soil allowing for potential decontamination through the removal of the soil surface

349  (e.g. top 5 cm) in undisturbed sites. Further, as radiocesium is strongly fixated to fine mineral soils, it

350  potentially may be eroded during rainfall events and its migration and transfer from hillslopes to the

351  Pacific Ocean will be governed by the geomorphological and hydrological factors driving soil erosion,

352  mobilization, and transport processes.

353  **2. Radiocesium hillslope transfers**

354  As radiocesium is tightly bound to soil particles, the transfer of soil-bound radiocesium can occur

355  with the physical mobilization of soil particles during erosion processes (Yoshimura et al., 2015a). The

356  amount of radiocesium wash-off generated by erosion processes is dependent upon the volume of

357  soil eroded and the radiocesium concentration in the soil, with the latter being dependent on the

358  amount of radiocesium within the soil (Yoshimura et al., 2015a). In the coastal catchments of the

359  Fukushima Prefecture, sheetwash erosion on cultivated slopes dominates, as slope gradients on

360  cultivated hillslopes are low and their length is insufficient to allow runoff to concentrate and

361  generate rills or gullies (Vandaele et al., 1996).

362  To examine soil and radiocesium export, Yoshimura et al. (2015a) established seven Universal Soil

363  Loss Equation (USLE) run-off plots in Kawamata Town. They examined one forest, two cultivated, two

364  uncultivated, and two grassland sites and reported that land use is important when modelling the

365  export of radiocesium. In particular, one uncultivated farmland plot dominated the radiocesium and

366  sediment runoff. The farmland plots had the highest rates of erosion (1 kg m$^{-2}$ of soil loss) and $^{137}$Cs

367  export (16 kBq m$^{-2}$), followed by grassland and the forest plots (< 0.1 kg m$^{-2}$ of soil loss and < 2 KBq m$^{-2}$

368  $^{2}$ of $^{137}$Cs). In particular, Yoshimura et al. (2015a) reported an exponential relationship between

369  vegetation cover and soil loss.

370    Quantifying hillslope erosion is difficult for Japanese paddy fields as they may be both sources and

371    sinks of sediment and sediment-bound radiocesium (Tanaka et al., 2013b; Wakahara et al., 2014).

372    When paddies are puddled for the rice growing season, they are flooded with water potentially

373    containing suspended sediment and adsorbed radiocesium (Endo et al., 2013; Wakahara et al., 2014;

374    Yoshikawa et al., 2014). Further, when the paddies are drained, they are directly connected to the

375    stream network and may become a significant source of sediment and radiocesium, as water and

376    sediments discharged from paddy fields are often transferred directly to stream systems (Wakahara

377    et al., 2014).

378    Tanaka et al. (2013b) investigated the impact of contaminated irrigation water on rice paddy

379    radiocesium inventories. Although they did not report a significant impact of irrigation water on the

380    radiocesium inventory in the paddy, they concluded that significant rainfall events may increase

381    radiocesium migration and transfer. In a non-hillslope erosion oriented study, Yoshikawa et al. (2014)

382    found that the irrigation of paddy fields only contributed an additional 0.03-0.05% of $^{137}$Cs to the pre-

383    irrigation paddy field $^{137}$Cs inventory. The authors concluded that the additional $^{137}$Cs load from

384    irrigation is negligible in comparison to the existing soil $^{137}$Cs inventory.

385    Wakahara et al. (2014) examined the discharge of radiocesium from rice paddy fields reporting that a

386    normally cultivated paddy field exported 1240 Bq m$^{-2}$ of $^{137}$Cs after puddling and 102 Bq m$^{-2}$ after

387    irrigation. Comparatively, a decontaminated paddy exported 48 Bq m$^{-2}$ of $^{137}$Cs after puddling and

388    317 Bq m$^{-2}$ after irrigation. Although decontamination removed 95% of the fallout radiocesium from

389    this particular paddy, the export of radiocesium from the decontaminated paddy was greater after

390    irrigation than the non-decontaminated paddy. The authors concluded that water inflows during

391    events and irrigation with sediment-bound $^{137}$Cs contributed to this counter-intuitive result.

392    There has been limited research on the radiocesium migration from forests. Kitamura et al. (2014)

393    modelled that forest soils, which occupy a large portion of the region, export only a small fraction of

394    soil and radiocesium. Pratama et al. (2015) modelled that subcatchments of the Abukuma River with

395    greater proportions of forest coverage have the lowest radiocesium export. Nagao et al. (2013)

396    confirmed this finding in their monitoring research through indicating that, while forest land uses

397    cover 64% of their research catchments, they only accounted for 24% of soil and 41% of $^{137}$Cs export.

398    Although forests disproportionately contribute less radiocesium than their initial inventories, the

399    gross amounts exported are high owing to their large area (Kitamura et al., 2014).

400    Fig. 7 illustrates the limited extent of direct hillslope erosion sampling in the Fukushima region. The

401    research on hillslope erosion was located in the Abukuma catchment. This limited research reflects a

402    similar lack of research in monsoonal regions on soil erosion owing to the difficulties in conducting

403    complex field observation studies during intense rainfall conditions or replicating these conditions in

404    laboratory environments. More research at the hillslope scale is important to quantify the erosion

405    and concomitant radiocesium transfer during runoff events. Different erosion and runoff dynamics

406    exist for each land use, complicating our understanding of the detachment and transfer of

407    contaminated sediments, particularly in catchments with mixed land use (Kinouchi et al., 2015). As

408    radiocesium is bound to soil, its initial mobilization and transfer will be directly dependent on the

409    various factors governing soil erosion (for example see Morgan et al. (1998); Nearing et al. (1989);

410    Renard et al. (1991)). Thoroughly characterizing potential soil erosion processes from different

411    sources at the hillslope scale is thus fundamental to understanding the potential transfer from

412    hillslopes to the Pacific Ocean. In particular, more research is required to properly characterize the

413    dominant sources of particulate radiocesium in the Fukushima region and the relative contribution of

414    these sources to radiocesium fluxes to the Pacific Ocean.

415    **3.  Factors influencing riverine radiocesium transfer**

416    As radiocesium mobilized from hillslopes and transported downstream is selectively attached to the

417    finest eroded soil particles (Kinouchi et al., 2015), it is important to develop a quantitative

418    understanding of the particle size redistribution of radiocesium to predict potential contamination of

419    downstream areas that are more densely populated and not-affected by the initial fallout (Kinouchi

420  et al., 2015; Ueda et al., 2013). Characterizing the particle size distribution of radiocesium will

421  improve our understanding of the potential transfer of radiocesium (e.g. fine particle fractions
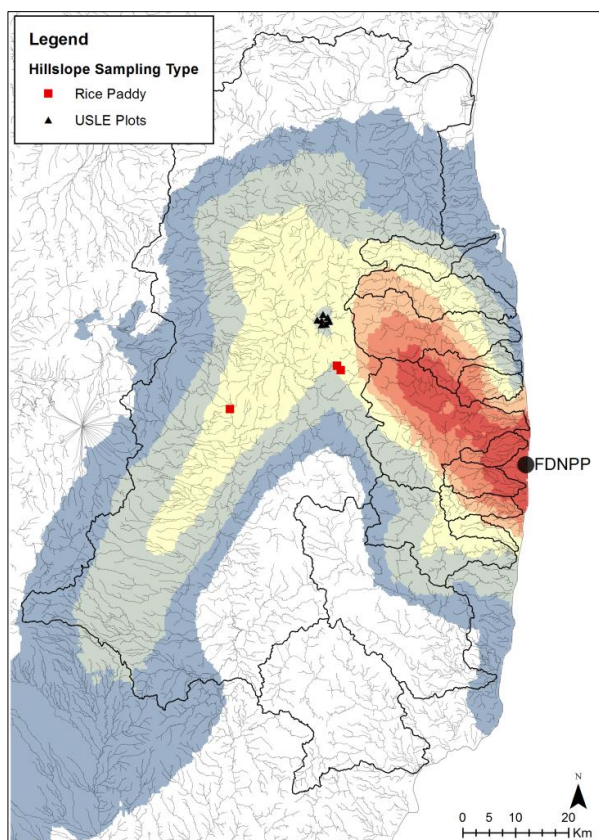


**Figure 7.** Sample locations for research examining hillslope radiocesium transfer with USLE-based and calculations of suspended sediment yields form rice paddy fields.

422  transfer farther and possibly stored longer) and also potential storage within stream systems (e.g.

423  coarse particles are deposited sooner). Along with the particulate fraction, it is important to

424  understand the dissolved/particulate partitioning of transported radiocesium in rivers and streams.

425  Radiocesium is transferred in both dissolved and particulate fractions that behave differently.

426  Examining the rainfall/climate is also important to determine the impacts of climate on radiocesium

427  transfer and storage. Importantly the potential storage of radiocesium between hillslopes and the

428  Pacific Ocean may become a significant focal point of future management efforts. Prior to examining

429  research that quantifies radiocesium transfers and export from the coastal catchments, each of these

430  dynamics impacting radiocesium transfers will be discussed.

431     In the fallout affected catchments, the main radioactive pollution plume is drained by the Abukuma

432     River, along with several small coastal catchments (Fig. 3). The majority of research has focused on

433     understanding the transfer of fallout contamination in the Abukuma River basin (Fig. 8). For the

434     smaller coastal catchments, there has been a focus of research in the Niida and Mano rivers with

435     decreasing research in the catchments close to and south of the FDNPP. In particular there has been

436     limited research published on the catchments with the highest mean radiocesium inventories (the

437     Maeda, Kuma, Ukedo and Ota catchments).
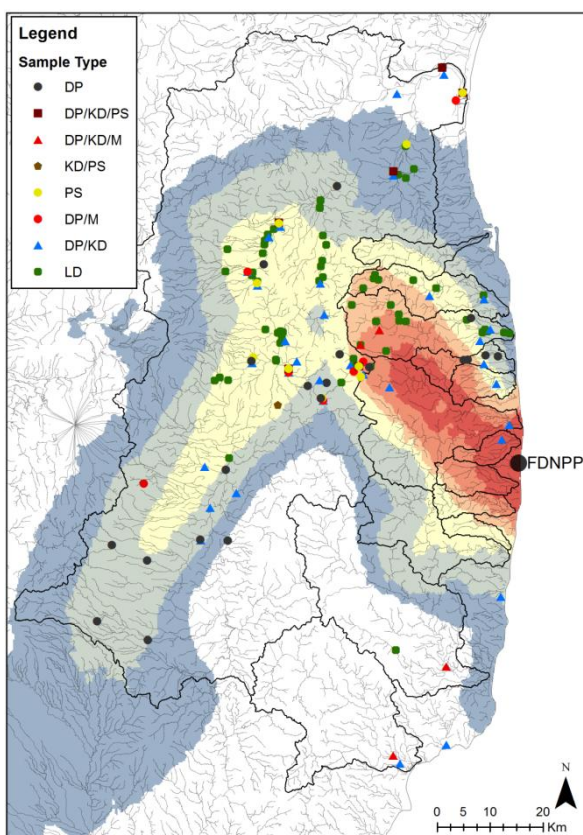


**Figure 8**. Location of stream sampling locations for samples examining dissolved/particulate (DP) fractions and their distribution coefficient (KD), particle size (PS), monitoring (M), and lag deposits (LD).

438     *4.1 Radiocesium distribution coefficient (dissolved/particulate)*

439     To quantify radiocesium migration in catchments, it is necessary to understand the ratio of

440     particulate and dissolved radiocesium transported in river systems. Dissolved and particulate-bound

441     radiocesium migrate differently in waterways and their ratio provides fundamental information for

442  understanding future migration (Yoshimura et al., 2015b). The dissolved/suspended partitioning of

443  radionuclides is typically described with a distribution coefficient, $K_d$, and is expressed as a ratio of

444  radiocesium activity concentration in particulate and dissolved fractions under equilibrium conditions

445  (Ueda et al., 2013).

446  In samples from the Abukuma River, Sakaguchi et al. (2015) reported that the particulate fraction

447  transported 80% of [137]Cs (Table 3). Conversely, Tsuji et al. (2014) indicated that in the Abukuma and

448  Ota catchments, only 64% of the radiocesium was transported with the particulate fraction. When

449  examining sediments across the fallout impacted region, Yoshimura et al. (2015b) found that

450  between 58-100% of radiocesium was transported with the particulate fraction, with the exclusion of

451  one estuary site. Similarly, Yoshikawa et al. (2014) reported that between 60-95% of radiocesium was

452  transported with the particulate fraction in three small subcatchments (<0.1 km²) of the Abukuma

453  River.

454  Differences between these results are likely related to the timing of sampling in relation to significant

455  rainfall events. For example, in the Same and Natsui catchments, Nagao et al. (2013) observed that in

456  normal flow conditions, the particulate fraction transported 40% of the ^{137}Cs, compared to ~100%

457  during a significant rainfall event (i.e. Typhoon Roke). Ueda et al. (2013) also reported significant

458  differences between flood and base flow conditions with the particulate partition contributing over

459  90% of radiocesium in the Niida River during Typhoon Roke. In this catchment, the particulate

460  fraction only accounted for 40% of the radiocesium migration in base flow conditions. In addition,

461  Shinomiya et al. (2014) found that 92-97% of radiocesium is transferred with the particulate fraction

462  during significant rainfall events (Typhoon Guchol), compared to between 12-96% in base flow. From

463  modelling research, Mori et al. (2014), determined that the particulate fraction transported more

464  than 95% of the ^{137}Cs, slightly above the range calculated by Yamashiki et al. (2014) (82-93%). This

465  research clearly demonstrates that the particulate fraction dominates the transfer of radiocesium in

466  the Fukushima region during major rainfall events.

467    Differences between the dissolved/particulate radiocesium partitioning may also be influenced by

468    the time elapsed since the FDNPP accident. For example, in the Niida catchment, Nagao et al. (2014)

**Table 3.** Summary of research examining radiocesium in particulate/dissolved and $K_d$

| Author(s) | Catchment(s) | Sampling Period | Radionuclide(s) | Particulate Fraction of transported $^{137}$Cs (%) | Average K(d) |
|---|---|---|---|---|---|
| Nagao et al. (2013) | Same / Natsui | July 2011 - Dec. 2011 | $^{134}$Cs & $^{137}$Cs | 99 Flood Conditions<br>33 Base Flow | $2.5 \times 10^6$ |
| Nagao et al. (2014) | Niida | May 2011 - Nov. 2012 | $^{134}$Cs & $^{137}$Cs | 47 (Before Sept. 2011)<br>84 (After Sept. 2011) | N/A |
| Sakaguchi et al. (2015) | Abukuma | June 2011 - Dec. 2012 | $^{137}$Cs | 80 | $8.8 \times 10^5$ |
| Shinomiya et al. (2014) | Experimental Catchment (Abukuma) | June 2012 | $^{134}$Cs, $^{137}$Cs | 92-97 Flood Conditions<br>12-96 Base Flow | N/A |
| Tsuji et al. (2014) | Abukuma, Ota | Sept. 2012 - May 2013 | $^{134}$Cs & $^{137}$Cs | 64 | N/A |
| Ueda et al. (2013) | Niida | July 2011 - Nov. 2011 | $^{134}$Cs & $^{137}$Cs | >90 Flood Conditions<br>40 Base Flow | $3.5 \times 10^5$ |
| Yamashiki et al. (2014) | Abukuma | June 2011 - May 2012 | $^{134}$Cs & $^{137}$Cs | 82-93 | N/A |
| Yoshikawa et al. (2014) | Abukuma | April 2012 – Sept. 2012 | $^{137}$Cs | 60–83 Flood Conditions<br>69–95 Base Flow | $1.2 \times 10^5$ Base<br>$10.6 \times 10^5$ Event |
| Yoshimura et al. (2015b) | Abukuma, Mano, Same, Fujiwara, Niida, Ota, Odaka, Asami, Ukedo, | Dec. 2012 | $^{134}$Cs & $^{137}$Cs | 58-100[a] | $3.6 \times 10^5$ |

[a] excluding an estuary site.

469    reported that the particulate fraction averaged 47% between May and September 2011 compared to

470    84% between December 2011 and November 2012. The differences were attributed to rainfall and

471    declining availability of leachable sources of radiocesium that were likely washed off in greater

472    concentrations early after the accident. When researching dissolved radiocesium fractions in stream

473    and ground water, Iwagami et al. (Submitted) also reported a fast flush of radiocesium before

474    October 2011, resulting from the initial wash-off, followed by a slow decline in radiocesium

475    concentrations.   Moving forward, it is likely that the particulate phase will constitute a greater

476    proportion of the radiocesium transfer.

477    In the Niida catchment, Ueda et al. (2013) reported that the mean $K_d$ was $3.5 \times 10^5$ (Table 3).

478    Yoshimura et al. (2015b) calculated a very similar mean $K_d$ of $3.6 \times 10^5$ when comparing the

479    particulate material sampled from time-integrated samplers (Phillips et al., 2000) and water sampled

480    with a vacuum pump sampler. Nagao et al. (2013) demonstrated that the $K_d$ range in the Same and

481    Natsui Rivers was between $0.4 \times 10^6 - 5.0 \times 10^6$. Yoshikawa et al. (2014) reported that the $K_d$ in three

482    small (<1.2 km²) was $1.2 \times 10^5$ in base flow compared to $10.6 \times 10^5$ in event conditions. Sakaguchi et

483    al. (2015) indicated the $K_d$ in the Abukuma River was $8.8 \times 10^5$. In general, these results are an order

484    of magnitude greater than those reported by the International Atomic Energy Agency after the

485    Chernobyl accident ($2.9 \times 10^4$) (UNSCEAR, 2000) indicative of a greater percentage of particulate-

486    bound radiocesium migrating through these catchments compared to those sampled in areas

487    impacted by fallout from the Chernobyl accident. In Ukrainian rivers with similar volumes of total

488    suspended solids as in Fukushima rivers, the dissolved fraction was found to contain ~75% of the

489    sampled [137]Cs (1-2 y post-accident) (Sansone et al., 1996). Although a significant component of

490    radiocesium migrates with the dissolved fraction in normal flow conditions in the Fukushima region,

491    it contributes only a limited amount to the total radiocesium migration to downstream areas

492    (Kinouchi et al., 2015). The challenge is that the particulate radiocesium concentrations are often

493    irregular and driven by suspended solid fluctuations resulting from heavy precipitation (Tsuji et al.,

494    2014) and it is difficult and costly to continuously monitor suspended solids, particularly during high

495    flow conditions.

496    Ueda et al. (2013) demonstrated a high correlation between the discharge of radiocesium and fluvial

497    water discharge. Correlations were also found between particulate/dissolved radiocesium

498    concentrations and catchment radiocesium inventories, suggesting that it may be possible to predict

499    radiocesium concentrations (Yoshimura et al., 2015b). As this correlation is empirical and may

500    change owing to regional hydro-meteorological dynamics, further research is required before using

501    this relationship directly in modelling approaches. Importantly, $K_d$ was found to be related to the

502    proportion of large particles (e.g. low clay content), the clay mineralogy of small particles, and the

503    aqueous phase cation concentration (Fan et al., 2014a). As radiocesium primarily bound to fine

504    sediment particles (Yamaguchi et al., 2012), it is important to understand the relationship between

505    radiocesium and particle size for modelling radiocesium transfer at larger scales.

506    ***4.2 Radiocesium particle size distributions***

507    The fine soil fraction, to which radiocesium is bound, is preferentially eroded at the hillslope scale

508    (mean particle size = 25.5 μm) (Yoshimura et al., 2015a). This fraction (e.g. silt and clay) is also

509    preferentially transported farther distances owing to a smaller settling velocity (Iwasaki et al., 2015)

510    resulting in the accumulation of radiocesium in downstream areas potentially unaffected by the

511    initial fallout (Tanaka et al., 2014). Indeed the distribution of radiocesium with regards to particle size

512    will have a significant impact on the radiocesium deposition in downstream areas. It is therefore

513    important to examine whether sediment generation and transport processes impact the radiocesium

514    fixation to fine particles.

515    River sediments were found to have a high ^{137}Cs adsorption capacity (Fan et al., 2014a). Multiple

516    studies demonstrated that radiocesium concentrations were elevated in the fine particle size

517    fractions (Fan et al., 2014a; Sakaguchi et al., 2015; Tanaka et al., 2015; Tanaka et al., 2014). Sakaguchi

518    et al. (2015) found that the maximum ^{137}Cs concentration in suspended sediment was found in the

519    silt particle size fraction (3-63µm). This result was also reported in Fan et al. (2014a). In the former

520    case, $^{137}$Cs in each fraction did not demonstrate any systematic variation across multiple sampling

521    sites (Sakaguchi et al., 2015). In the latter, Fan et al. (2014a) found that there was a weak relationship

522    between particle size and radiocesium for fine sediment (<63 µm), though a stronger relationship

523    was derived for the coarser grain fractions (e.g. >63 µm).

524    The sorption of radiocesium to sediments was found to be directly related to their physical-chemical

525    properties, including cation exchange capacity, organic matter content and mineralogy (Fan et al.,

526    2014a). What was unexpected with these findings was that the radiocesium concentrations were not

527    always enriched in the fine clay material (<3 µm). A below expected quantity of radiocesium in the

528    fine clay material was also reported by Tanaka et al. (2014) who found that the silt and sand fractions

529    transported 95% of the sediment-sorbed radiocesium. This study did find an enrichment of $^{137}$Cs in

530    the clay material, though it was found to only constitute a small proportion of the sampled bedload

531    material. Fan et al. (2014a) also reported a low clay mineral content in the <2 µm particle size

532    fraction. The lack of radiocesium enrichment in the finest particle size fraction may be the result of

533    sampling technique (e.g. sampling bed load material) or other fluvial processes that may result in the

534    majority of very fine material being exported from the catchment.

535    For modelling and management of radiocesium transfers in the contaminated catchments, it may be

536    silt, rather than clay that requires emphasis. For example, silt was found to be the significant source

537    of bed contamination (excluding initial fallout) whereas during later stages of rainfall flow events,

538    clay materials were found to be the dominant supply of $^{137}$Cs to the lower river reaches (Kurikami et

539    al., 2014). Further characterization of the relationship between radiocesium and particle size is

540    fundamental for understanding radiocesium transfer and storage in fallout affected catchments.

541    ***4.3 Radiocesium mobilization: Rainfall regime***

542    Rainfall is the driving mechanism behind soil erosion by water (Nearing et al., 1989; Wischmeier and

543    Smith, 1958). The regional climate in conjunction with the topography of the fallout impacted region

544     exacerbates radiocesium transfer. The catchments of the Fukushima Prefecture are mountainous and

545     characterized with a steep topography (Kinouchi et al., 2015; Minoura et al., 2014). The

546     temperate/monsoonal climate results in high seasonal and annual precipitation including significant

547     runoff events generated from snowmelt and intense rainfall from typhoons (Evrard et al., 2013;

548     Yamashiki et al., 2014). In the Fukushima region, the annual precipitation is three-fold greater than in

549     Chernobyl, resulting in a more rapid radiocesium washoff (Tsuji et al., 2014). This climate is one of

550     the fundamental mechanisms driving the migration and transfer of radiocesium throughout the

551     catchments that received the original fallout (Evrard et al., 2013).

552     Evrard et al. (2013) demonstrated that the region is highly reactive to both rainfall and snow fall

553     events. The authors demonstrated that there is a significant export of contaminated material from

554     coastal rivers to the Pacific Ocean. Chartin et al. (2013) found that the combination of rainfall and

555     snowmelt events results in a progressive migration of sediment bound radiocesium to the Pacific

556     Ocean. This sediment-based sampling clearly demonstrated that there has been a significant

557     dispersion of contaminated sediments in the 20 months after the FDNPP accident (Chartin et al.,

558     2013). These authors highlight a massive, rapid and episodic transfer of radiocesium resulting from

559     the climate in general and the snowmelt/typhoon cycle in particular. Yamashiki et al. (2014) also

560     reported two significant runoff peaks in their research, one clearly coinciding with the snowmelt in

561     late spring (April-May) and the other coinciding with typhoons.

562     Overall, the literature clearly demonstrates that the majority of soil erosion and concomitant

563     radiocesium migration, coincides with extreme rainfall-runoff events (Minoura et al., 2014; Mouri et

564     al., 2014; Nagao et al., 2013; Onishi et al., 2014). In fact, most sediment and radiocesium migration is

565     thought to occur during short flood events that may occur 1-2 times per year (Yamaguchi et al.,

566     2014). This importance of flooding and rainfall was incorporated by Kitamura et al. (2014) who only

567     modeled sediment migration when the flow rate is 10 times greater than the average annual flow.

568 In particular, the typhoons in the fallout impacted region transfer massive amounts of sediment and

569 radiocesium. For example, Typhoon Roke (Sept. 2011) destroyed paddy banks (Wakahara et al.,

570 2014) and resulted in mud depositions that were ~10 cm thick (Minoura et al., 2014). Yamashiki et al.

571 (2014) estimated that Typhoon Roke mobilized and transferred 6.18 TBq, or 61% of the total

572 radiocesium load to the coastal areas during their observation period. Kinouchi et al. (2015) reported

573 that three major flow events were responsible for the migration of 43% of the sediment between

574 June 2011 and Dec. 2012. Nagao et al. (2013) demonstrated that radiocesium concentrations were

575 an order of magnitude higher during high flow conditions after Typhoon Roke, which also resulted in

576 particulate transport of radiocesium being 100% compared to 21-56% in baseflows. The authors

577 concluded that these heavy rainfall events are one of the important drivers of radiocesium migration

578 from catchments to the coast resulting for between 30-50% of the annual radiocesium coastal

579 transfer. Ultimately, extreme rainfall events are fundamental to the migration of sediments and

580 radiocesium from the hillslopes to the Pacific Ocean.

581 *4.4 Radiocesium storage: Reservoirs and dams*

582 Not all mobilized sediment and radiocesium is exported to the Pacific Ocean. The migration of

583 sediment, particularly coarse particle size fractions, occurs over longer temporal scales. Further,

584 anthropogenic alterations to riverine morphology, such as reservoirs and dams, further delay the

585 migration and transfer of sediment and radiocesium downstream (Kurikami et al., 2014). Reservoirs

586 not only delay the migration of radiocesium and sediments, they also may act as a major sinks and

587 storage (Evrard et al., 2014a; Evrard et al., 2013) as only a select fraction of radiocesium is

588 transferred downstream, predominantly the dissolved or clay-bound fractions (Onishi et al., 2014).

589 These reservoirs may also act as sources of contaminated sediment during water releases.

590 Chartin et al. (2013) reported a significant layer of sediments with high radiocesium concentrations

591 deposited behind a reservoir in the upper Ota River. Kitamura et al. (2014) indicated that $10^4$ t of

592 sediment and 10 TBq of $^{137}$Cs were transferred into the Ogaki Dam on the Ukedo River which

593 buffered the downstream transfer of radiocesium. Kurikami et al. (2014) reported that the sand

594 particle size fraction was completely contained within the Ogaki Dam, with only 5% of the silt and

595 50% of the clay fractions transferred downstream. Similarly, Yamada et al. (2015) found that

596 practically all of the silt and sand are deposited within the Ogaki Dam reservoir, with the sand being

597 deposited near the entrance of the reservoir and the silt being more uniformly distributed.

598 Approximately a third of the clay fraction was modelled to be exported downstream from this

599 reservoir (Yamada et al., 2015).

600 Management of the dams and reservoirs may have a significant impact on radiocesium migration

601 downstream. Mouri et al. (2014), Yamada et al. (2015) and Kurikami et al. (2013) demonstrated that

602 reservoir management could assist in the control of radiocesium fluxes. The challenge with the

603 management of these reservoirs in the temperate/monsoonal climate in the Fukushima region is that

604 occasional water releases are required for their safe operation. Evrard et al. (2014a) indicated these

605 dam releases could enhance the natural migration of radiocesium downstream and may become a

606 significant factor controlling the downstream transfer of sediment and radiocesium in these

607 anthropogenically modified catchments. In the Fukushima Prefecture, there are 10 significant dams

608 and over a 1,000 reservoirs for both agricultural and surface water management (Yamada et al.,

609 2015). Understanding the radiocesium deposition and migration within these water storages is

610 important for understanding potential contamination of downstream regions, particularly cultivated

611 rice paddy systems.

612 To quantify radiocesium transfer from hillslopes to the Pacific Ocean, it is necessary to characterize

613 riverine radiocesium dynamics within the climatic context. Radiocesium may be transferred in

614 particulate or dissolved fractions, and the particle size distribution of particulate radiocesium will

615 either facilitate its transfer or potential downstream storage during rainfall and snowmelt runoff

616 events that drive the majority of radiocesium migration. Understanding these dynamics, particularly

617 in the catchments with the highest mean radiocesium activities will be of increasing importance

618    moving forward. In particular, characterizing interrelationships between typhoons and other

619    rainfall/runoff events along with radiocesium particle size and distribution coefficients allows

620    researchers to determine whether radiocesium may be stored within a catchment after its hillslope

621    mobilization or whether it is ultimately transferred to the Pacific Ocean.

622    ***4. Quantifying radiocesium transfers from hillslopes to the Pacific Ocean***

623    Radiocesium dynamics within riverine environments are inherently complex. Accordingly, there are a

624    variety of factors governing radiocesium transfer in the region affected by the FDNPP accident.

625    Quantifying radiocesium transfers requires in-stream sampling and monitoring stations or complex

626    desktop sediment modelling. Publications reviewed for this section focus on catchment scale

627    radiocesium transfers and will be subdivided into monitoring and modelling research. Table 4 lists

628    these two approaches to quantifying radiocesium transfers in the Fukushima coastal catchments

629    while Fig. 8 includes the locations of the monitoring stations. Similarly to the research on the factors

630    influencing riverine radiocesium transfers above, the majority of modelling research occurs within

631    the Abukuma River catchment. There is limited monitoring and modelling research in the smaller

632    coastal catchments, particularly the catchments to the south and in close proximity to the FDNPP.

633    ***5.1 Monitoring radiocesium catchment scale transfers***

634    Direct monitoring of radiocesium sampled within rivers over several months or years provides data

635    required to quantify radiocesium exports from catchments. For example, relationships between total

636    suspended solid and radiocesium quantities within river water/sediment samples may be quantified

637    and extrapolated over longer temporal periods. Although there are limitations, this monitoring

638

**Table 4.** Summary modelling and monitoring results

| Author(s) | Type | Catchment(s) | Area (km$^2$) | Period | Radionuclides (Particulate (P)- Dissolved (D)) | Export (TBq) | Catchment Inventory Exported (%) |
|---|---|---|---|---|---|---|---|
| Iwasaki et al. (2015) | Modelling | Abukuma (downstream reach) | 31 | September 2011 | $^{137}$Cs (P) | 3.29 | n/a |
| Kinouchi et al. (2015) | Modelling | Abukuma (Kuchibuto subcatchment) | 140 | June 2011 - December 2012 | $^{137}$Cs (P) | 0.274 | 0.8 |
| Kitamura et al. (2014) | Modelling | Abukuma, Ukedo, Niida, Maeda, Kuma, Ota, Mano, Kido, Odaka, Tomioka, Natsui, Same, Ide, Uda | 8,352 | Annually for the initial years after the accident | $^{137}$Cs (P) | 8.4 | 1.0 |
| Kurikami et al. (2014) | Modelling | Ukedo (Okagi Dam) | n/a | September 2013 | $^{137}$Cs (D&P) | 0.86[a] | n/a |
| Mori et al. (2014) | Modelling | Un-named reservoir | 15 | March 2011 - December 2013 | $^{137}$Cs (P) | n/a | <5.0 |
| Mouri et al. (2014) | Modelling | Tone (Kusaki Dam) | 254 | 2010 - 2090 | $^{137}$Cs (P) | 900 Bq/kg[b] | n/a |
| Nagao et al. (2013) | Monitoring | Natsui, Same | 749/600 | March 2011 - December. 2011 | $^{134}$Cs, $^{137}$Cs (D&P) | 0.04 | n/a |
| Pratama et al. (2015) | Modelling | Abukuma | 5,172 | August 2011-May 2012 + future scenarios | $^{134}$Cs, $^{137}$Cs (D&P) | ~12 | 2% |
| Shinomiya et al. (2014) | Monitoring | Experimental Catchment (Abukuma) | 0.01 | June 2012 | $^{134}$Cs, $^{137}$Cs | 115 (Bq m$^2$) | 0.07 |
| Ueda et al. (2013) | Monitoring | Niida (Wasriki and Hiso Rivers) | < 5 | July-November 2011 | $^{134}$Cs, $^{137}$Cs (D&P) | 0.03 | 0.4 |
| Yamada et al. (2015) | Modelling | Ukedo (Okagi Dam) | n/a | September 2013 & average flood | $^{137}$Cs (D&P) | 0.07 & 0.35 | n/a |
| Yamaguchi et al. (2014) | Modelling | Abukuma, Ukedo, Niida, Maeda, Kuma, Ota, Mano, Kido, Odaka, Tomioka, Natsui, Same, Ide, Uda | 8,352 | March 2011 - March 2012 + future scenarios | $^{137}$Cs (P) | 02.3 - 6.5[c] | 0.5 - 7.5[c] |
| Yamashiki et al. (2014) | Monitoring | Abukuma | 5,172 | June 2011 - May 2012 | $^{134}$Cs, $^{137}$Cs (P) | 10.08 | 1.1 |

[a] deposited in the Okagi Dam
[b] current annual deposition in the Kusaki Dam modelled to be ~900 Bq/kg
[e] minimum and maximum values modelled over 30 y

639    approach is a direct method to quantify radiocesium transfer from catchments and ultimately to the

640    Pacific Ocean.

641    Most of the direct radiocesium monitoring within catchments occurs at the smaller subcatchment

642    scale. For example, Shinomiya et al. (2014) monitored radiocesium discharge from a small forested

643    catchment (0.012km$^2$) in Abukuma River basin. The authors found that maximum rainfall intensity

644    and runoff coincided with the maximum radiocesium (3.9 Bq L$^{-1}$) and suspended solid export. During

645    the receding limb of the hydrograph, radiocesium transfers concentrations dropped sharply. In total,

646    115 Bq m$^{-2}$ was exported from this experimental catchment or 0.07% of the initial radiocesium

647    inventory, indicative of a negligible radiocesium transfer from this forested catchment during a

648    typhoon event.

649    Ueda et al. (2013) conducted regression analyses to relate radiocesium to river discharge at two

650    sampling locations in the upper Niida catchment between March 15 and December 31, 2011. They

651    estimated that 0.045 TBq and 0.020 TBq were exported from the Hiso and Wariki Rivers catchments,

652    respectively. This equated to 0.5% of the radiocesium inventory of the Hiso catchment and 0.3% of

653    the Wariki River catchment. Although each catchment had different land uses, their proportional

654    radiocesium export were similar.

655    Nagao et al. (2013) calculated radiocesium export from the Natsui and Same Rivers catchments,

656    south of the FDNPP. They quantified radiocesium flux by multiplying mean monthly discharge by the

657    $^{137}$Cs concentrations and time. They determined that 0.003 and 0.005 TBq y$^{-1}$ of $^{137}$Cs were exported

658    from the Natsui and Same Rivers, respectively. They also indicated that 30-50% of their estimated 10

659    month $^{137}$Cs export occurred during Typhoon Roke.

660    To our knowledge, there has only been one current study published quantifying the transfer of

661    radiocesium from a large catchment to the Pacific Ocean. Yamashiki et al. (2014) used in-stream

662    samplers to collect suspended sediment along with turbidity meters and pressure transducers to

663    calculate suspended sediment fluxes from the Abukuma River catchment to the Pacific Ocean. The

664    authors estimated that ~10 TBq of radiocesium was exported to the Pacific between June 2011 and

665    May 2012. This amounted to ~1% initial estimated catchment inventory. This direct transfer of

666    sediment from hillslopes through the Abukuma catchment to the Pacific Ocean was within the same

667    order of magnitude of the direct leakage from the FDNPP to the ocean on August 21, 2013 (24 TBq)

668    (Yamashiki et al., 2014) clearly demonstrating the importance of quantifying the riverine transfer of

669    radiocesium to the Pacific Ocean.

670    *5.2 Modelling radiocesium catchment scale transfers*

671    Quantifying catchment scale radiocesium transfers with modelling approaches requires a variety of

672    model inputs along with calibration and validation data (often obtained from direct river monitoring).

673    The challenge for researchers when quantifying catchment radiocesium fluxes is incorporating the

674    fundamental radiocesium transfer dynamics required to populate models without over

675    parameterizing radiocesium dynamics. Often, the scale of the research catchment controls the

676    breadth of radiocesium dynamics incorporated into individual models. Similarly to the monitoring

677    studies, desktop models have been performed at various scales, from upstream catchments to large

678    river basins to quantify radiocesium transfer directly to the Pacific Ocean.

679    For an upstream catchment of the Abukuma River system, Kinouchi et al. (2015) developed a

680    complex model incorporating evaporation, evapotranspiration, infiltration, surface and subsurface

681    runoff along with groundwater, overland and river flow. The authors coupled hydrological processes

682    and energy transfer within a catchment along with interactions between surface water and

683    groundwater. Importantly, they modelled the hydrological processes for paddy fields, including

684    irrigation, ponding, drainage and seepage to nearby channels. Their model also incorporated season

685    variation in vegetation. The authors reported that after 30 y, the catchment inventory of $^{137}$Cs will be

686    reduced to 39% of the initial inventory (Kinouchi et al., 2015). They reported that between

687    September 2011 and December 2012, 0.274 TBq of $^{137}$Cs was exported from the Kuchibuto River

688    catchment or less than 1% of the initial $^{137}$Cs fallout.

689    Several studies modelled sediment and radiocesium deposition in reservoirs of the region. Mouri et

690    al. (2014) examined radiocesium inputs to the Kusaki Dam reservoir on the edge of the fallout

691    affected region. The authors incorporated mixed-particle size distributions into a sediment transport

692    equation to determine sedimentation and concomitant $^{137}$Cs deposition in the reservoir. The authors

693    included 10 different particle size fractions into their model. They reported that the wash load

694    (particle size ≤0.2mm) contributed little to reservoir siltation and predicted that 3.4 Mt/y of sediment

695    were deposited in the catchment with 900 Bq/kg of $^{137}$Cs. For the future, they predicted that

696    sediment deposition would increase to ~3.65 Mt/y with $^{137}$Cs activities of 120 Bq/kg.

697    Mori et al. (2014) modelled $^{137}$Cs dynamics in an unnamed reservoir catchment between March 2011

698    and December 2013. In particular, they developed an integrated model incorporating fully coupled

699    radionuclide behaviour in a channel, overland and subsurface three dimensional (3D), physics-based

700    model. The authors demonstrated that the majority of radiocesium was transported with the

701    particulate fraction (>95%). Their 3D model indicated that radiocesium was predominantly eroded

702    from steep hillslopes in close proximity to the stream network with the majority of deposition

703    occurring at the entrance of the reservoir. The authors determined that the total $^{137}$Cs discharge with

704    both sediment and dissolved fractions was <5% of the initial fallout inventory indicating the majority

705    of the fallout radiocesium remained in the dammed catchment.

706    Kitamura et al. (2014) reported the results from the application of the Time-dependent One-

707    dimensional Degradation and Migration (TODAM) model in the Ukedo Catchment. This model is also

708    outlined in Kurikami et al. (2014) and discussed in Kitamura et al. (2015). The TODAM model

709    incorporates the deposition and re-suspension of sediment along with the potential

710    desorption/adsorption of radiocesium within sub-models. It simulates the movement of three

711    sediment particle size fractions (sand/silt/clay). The authors determined that $^{137}$Cs concentrations

712    were lower than the drinking water limit after approximately 4 d following a significant rainfall event

713    (Kurikami et al., 2014). The authors also reported that 0.86 TBq of $^{137}$Cs was deposited in the Okagi

714    Dam Reservoir (Kitamura et al., 2014), which is only one order of magnitude less than the total $^{137}$Cs

715    export to the Pacific Ocean from 14 coastal catchments.

716    Yamada et al. (2015) also modelled radiocesium dynamics for the Ogaki Dam with the Nay2D model

717    (Shimizu, 2003) to examine the influence of countermeasures such as controlling the reservoir

718    volume on $^{137}$Cs export. This paper was also discussed in Kitamura et al. (2015). The authors

719    compared a September 2013 flood event to the long-term average flood event and calculated $^{137}$Cs

720    deposition and export.  For the September 2013 flood, they modelled that 0.16 TBq was deposited in

721    the Ogaki Dam with 0.07 TBq exported downstream. These transfers were low compared to the

722    average yearly flood which was modelled to deposit 0.55 TBq and export 0.35 TBq.

723    Finally, several studies quantified the export of radiocesium from catchments to the Pacific Ocean by

724    focusing on lower river reaches or by modelling major catchments affected by fallout. Iwasaki et al.

725    (2015) investigated $^{137}$Cs dynamics in a downstream reach of the Abukuma River. They incorporated

726    a Rouse number threshold within their complex model to determine whether sediments are

727    exported from the reach or deposited. The authors reported there is significant deposition of

728    contaminated sediments on river floodplains. The authors highlighted the potential of using a Rouse

729    number threshold to determine the location of radiocesium deposition within the catchment to

730    target decontamination activities. In particular, they suggested that the floodplains and inner areas

731    of river bends can be contaminated at the end of significant rainfall events. Even whilst incorporating

732    deposition within the 31 km reach, the authors reported that 98% of $^{137}$Cs (or 3.2 TBq) was

733    transferred downstream towards the Pacific Ocean.

734    For the entire Abukuma River catchment, Pratama et al. (2015) developed a multiple compartmental

735    model that incorporated the complexity of radiocesium export from forest, urban and agricultural

736    land uses. The authors' model accurately predicted seasonal patterns of radiocesium fluxes in the

737    Abukuma catchment. The model was calibrated with monitoring data between August 2011 and May

738    2012 and then forecasted radiocesium migrations for the next 100 y. The authors found that in total

739 155 TBq of radiocesium will be exported from the Abukuma catchment over the next century. Based

740 on their results, approximately 12 TBq of radiocesium was modelled to be exported from the

741 Abukuma basin in the first year after the accident representing on average 2% of the initial

742 catchment inventory.

743 Kitamura et al. (2014) outlined an USLE-based model to estimate the ^{137}Cs discharge from 14

744 catchments that received fallout which are all outlined in Fig. 3. In particular, they focused on land-

745 use as they argued it may have the greatest potential impact on soil erosion. This model is also

746 described in Yamaguchi et al. (2014) and discussed in Kitamura et al. (2015). These authors reported

747 that 8.4 TBq of ^{137}Cs will be exported to the Pacific Ocean in the immediate years following the

748 FDNPP accident (Kitamura et al., 2014). This transfer of radiocesium to the Pacific Ocean can be

749 compared to estimates of direct radiocesium discharge from the FDNPP between June 2011 and

750 September 2012 (17 TBq), and a leakage event in August 2013 (24 TBq)(Kitamura et al., 2014;

751 Yamaguchi et al., 2014). The model also estimates that only 35% of eroded soils are transported to

752 the Pacific Ocean along with less than 1% of the initial radiocesium catchment inventory (Kitamura et

753 al., 2014).

754 *5.3 Monitoring and modelling summary*

755 A convenient approach to examine radiocesium transfer results is to compare the percentage of

756 initial radiocesium catchment inventory exported or remaining. At the plot or hillslope scale,

757 Yoshimura et al. (2015a) determined that between 0.07 and 3.2% of the catchment ^{137}Cs inventory

758 was exported with wash-off, with a mean annual export of 0.7% for their 7 USLE plots. For a forested

759 experimental catchment, Shinomiya et al. (2014) reported that only 0.07% of the initial radiocesium

760 inventory was exported during a typhoon event. In an outline of Fukushima related research

761 projects, Saito and Onda (2015) indicated that less than 1% of the radiocesium inventory is

762 transferred from hillslopes and discharged from catchments.

763     This annual wash-off rate of less than 1% is similar to the catchment modelling results obtained at

764     the subcatchment and catchment scales. In the Kuchibuto subcatchment of the Abukuma River,

765     Kinouchi et al. (2015) reported that 0.8% of the initial fallout (or 0.28 TBq) was exported from the

766     catchment. For the entire Abukuma catchment, Yamashiki et al. (2014) found that 1.1% of the

767     radiocesium inventory was exported to the Pacific Ocean compared to an average of 2% reported by

768     Pratama et al. (2015). In the upper Niida catchment, Ueda et al. (2013) reported that 0.3 to 0.5% of

769     the initial catchment radiocesium fallout was exported. For all 14 coastal catchments, Kitamura et al.

770     (2014) reported 99% of the catchment inventory remained with only 1% of the original fallout being

771     exported. The highest ^{137}Cs export compared to catchment inventory of <5% was modelled by Mori

772     et al. (2014). Although there is a significant amount of radiocesium exported from hillslopes and

773     catchments, this amount represents only a small fraction of the initial fallout inventory. Importantly,

774     comparing research results through using the percentages of catchment inventories remaining and

775     exported normalizes the results for comparison by removing the influences of catchment area, scale

776     of research, or even the simply different approaches to quantifying catchment inventories.

777     Although they did not estimate discharge, Chartin et al. (2013) clearly demonstrated that the

778     catchments that received fallout will become a perennial supply of radiocesium to the Pacific Ocean.

779     This was confirmed by the modelling research reviewed above with significant volumes of

780     radiocesium modelled to be exported annually from the fallout-affected catchments to the Pacific

781     Ocean. In total, for the entire region, this amount was estimated to be 6.9-10 TBq by both sample-

782     based (Yamashiki et al., 2014) and desktop modelling (Kitamura et al., 2014; Yamaguchi et al., 2014).

783     Iwasaki et al. (2015) modelled that 3.3 TBq of the ^{137}Cs export migrated through the lower reaches of

784     the Abukuma River alone during Typhoon Roke. After the Abukuma River, (Kitamura et al., 2014)

785     found that the Ukedo and Niida River catchments were the only catchments to export >1 TBq of

786     [137]Cs. Indeed, these coastal catchments will be significant long-term source of radiocesium to the

787     Pacific Ocean.

788  Confirming the terrestrial origin of radionuclides detected in sediment collected in the Pacific Ocean

789  is particularly difficult. Several origins are possible: previous deposits associated with atmospheric

790  bomb testing in the 1960s; direct releases from FDNPP to the ocean; and exports from coastal rivers

791  of Eastern Japan. In order to quantify the respective contributions of these sources, the

792  measurement of additional radionuclides in marine sediment may provide indications on their origin.

793  For instance, a study showed that material exported by rivers draining the Fukushima radioactive

794  pollution plume was characterised by a different $^{239}$Pu/$^{241}$Pu atom ratio than the material originating

795  from areas of Japan devoid of Fukushima fallout (Evrard et al., 2014b). Alternatively, the detection of

796  the shorter-lived $^{134}$Cs isotope in marine sediment indicates the presence of Fukushima fallout at this

797  location, as $^{134}$Cs fallout originating from the 1960s atmospheric bomb fallout fully decayed (Bu et al.,

798  2013).

799  **5. Management and research implications**

800  Characterizing the transfer of sediment and particle-borne radiocesium is required to predict future

801  radiocesium dispersion in the Fukushima Prefecture and design and implement effective

802  countermeasures. Reviewing the processes and dynamics governing radiocesium transfer from

803  hillslopes to the Pacific Ocean provides not only a comprehensive depiction of the fundamental

804  factors driving radiocesium transfer, it also highlights future potential radiocesium management

805  challenges on one hand, and future research perspectives on the other.

806  In the fallout-affected areas, there has been a massive decontamination effort. Thousands of workers

807  are decontaminating rice paddy fields, grasslands, and entire villages. For soil decontamination, the

808  vegetation and litter are first removed followed by the removal of the topsoil. The impact of this

809  decontamination on sediment modelling and radiocesium transfer research is unknown. The

810  decontamination may temporarily increase the supply of radiocesium as the significant de-

811  vegetation/soil management interventions is likely to result in an increase in the supply of sediments

812  to riverine systems, as reported by Evrard et al. (2014a) and Lepage et al. (2014a) following

813    preliminary decontamination works in the Upper Niida River catchment. The question is whether the

814    elevated suspended sediment loads mobilized by the decontamination will have elevated

815    radiocesium quantities, be equivalent to pre-decontaminated levels, or be lowered through dilution

816    with non-contaminated sediment? Further, will the decontamination efforts reduce the transfer of

817    radiocesium from the hillslopes to the Pacific Ocean?

818    Examining the remaining catchment inventory from multiple studies provides a direct method to

819    compare multi-scale research in the region. Although a significant quantity of radiocesium is

820    exported from catchments to the Pacific Ocean, this amount represents only a small fraction of the

821    initial catchment inventory (<5%). Therefore, quantifying sediment (dis)connectivity is fundamental

822    to not only understanding radiocesium migration in these catchments though also for highlighting

823    potential areas that may accumulate and store radiocesium. The coastal plains, that remain

824    inhabited, potentially serve as a large buffer zone which could temporarily store radiocesium

825    transferred from the upstream forested, mountainous piedmont range. Floodplains and riparian

826    zones that were not directly impacted by the FDNPP accident may receive significant pulses of

827    radiocesium during flooding events that transfer contaminated sediment from upstream areas.

828    Accordingly, it is important to determine whether and where are any important storages of

829    radiocesium that need to be managed appropriately. The potential incorporation of Rouse number

830    threshold may help isolate locations of radiocesium deposition within the catchment to target

831    decontamination activities. After major typhoons, it may be necessary to analyse deposited material

832    in populated areas for radioactive contamination.

833    Perhaps the most critical potential sediment and radiocesium sink are rice paddy fields. Rice paddy

834    fields, depending on the time of year and hydrological environment, may be both sources and sinks

835    of radiocesium. The fertile soils of the Fukushima region make it important agriculturally. In

836    particular, paddy fields occupy approximately 70% of all farming area in the region (Wakahara et al.,

837    2014). Unfortunately, radiocesium may transfer into rice. Contamination of agricultural products

838 mainly occurs by direct absorption (from fallout or irrigation) or by root uptake resulting in long-term

839 contamination of crops. Contamination during irrigation is problematic as radiocesium adsorption

840 from water is more direct than adsorption from soil and many fields are irrigated by rivers

841 contaminated with dissolved and particulate bound radiocesium (Nemoto and Abe, 2013). Transfer

842 factors (TF) from soil to plant depend on vegetation properties. Endo et al. (2013) determined the TF

843 for different parts of the rice (Table 5) and concluded that contamination is principally concentrated

844 in the roots. Furthermore, the TF was significantly higher in samples collected closer to the paddy

845 fields water inlet (Yoshikawa et al., 2014). Quantifying the radiocesium and sediment transfer to and

846 from paddy fields is therefore a fundamental research question with a significant impact for both

847 human health and also for truly understanding the transfer of radiocesium throughout the fallout

848 affected region.

849 **Table 5**. Radiocesium transfer factor of different products collected after the FDNPP accident.

| Author(s) | Type | Number of samples | TF values |
|---|---|---|---|
| Endo et al. (2013) | Root (rice) | 3 | $0.39 \pm 0.08$ |
| | Straw (rice) | 12 | $0.09 \pm 0.02$ |
| | Ear (rice) | 3 | $0.02 \pm 0.01$ |
| | Brown rice | 3 | $0.02 \pm 0.00$ |
| | Polished rice | 3 | $0.01 \pm 0.00$ |
| | Rice bran | 3 | $0.14 \pm 0.01$ |
| | Chaff (rice) | 1 | $0.05 \pm 0.01$ |
| Takeda et al. (2014) | Soybean grain | 46 | $0.09 \pm 0.11$ |
| Tazoe et al. (2012) | Mugwort | 6 | $0.02 \pm 0.01$ |
| | Clover | 1 | 0.03 |
| | Grass | 1 | 0.71 |

850 Understanding the storage of radiocesium within dams and reservoirs is important. As the

851 decontamination efforts remove significant inventories of radiocesium from low-to-medium

852 impacted areas, dams and reservoirs may present significant long-term radiocesium storages. These

853 reservoirs are not only major dams that provide water for the region, they also include hundreds of

854 smaller irrigation and farm dams. These dams could store significant quantities of radiocesium that

855 could be redistributed during a major flood event throughout the landscape potentially

856 contaminating, for example, previously decontaminated paddies.

857    Similarly, forests in the region will likely remain a significant long-term radiocesium reservoir.

858    Characterizing the storage and intra- and inter-forest radiocesium transfers will be necessary to

859    understand the transfer of radiocesium to and from forested hillslopes. This is important as forests

860    received the bulk of medium to high radiocesium fallout. Further, most of the forested communities

861    occur at high elevation on the coastal mountain ranges. Accordingly, they will likely act as a long-

862    term source of dissolved and particulate (including sediment bound and organic matter bound)

863    radiocesium. Forests may therefore contaminate downstream rice paddy fields, rural areas and

864    rivers, again including potentially recently decontaminated landscapes. Importantly, it will be

865    necessary to quantify radiocesium transfers from both deciduous and coniferous forests in order to

866    accurately quantify radiocesium transfers from hillslopes to the Pacific Ocean.

867    In general, more research is needed to quantify radiocesium mobilization and transfer at the hillslope

868    scale. In particular, a more detailed quantitative monitoring of soil erosion runoff under a variety of

869    land uses is necessary to improve our understanding of the generation and transfer of sediment

870    bound radiocesium at the hillslope scale, including the impact of different land uses (e.g. different

871    forests, rice paddy fields, rural residential and other cultivated landscapes). Direct monitoring of

872    hillslope erosion is necessary to ensure catchment scale models accurately reflect hillslope scale

873    erosion dynamics.

874    Along with a more accurate quantification of hillslope erosion dynamics, catchment scale models

875    require a rigorous incorporation of the regional climate along with the important drivers and

876    dynamics of radiocesium transfer from deposition zones. In particular incorporating the seasonality

877    of flooding events to coincide with changes in vegetation in the forest and rice paddy landscapes may

878    improve the quantification of radiocesium transfer in the region. In the fallout-impacted catchments,

879    most radiocesium is transported in particulate form, mainly during floods generated by typhoons or,

880    to a lesser extent, by snowmelt. Further research into this seasonal cycle is important to understand

881    radiocesium dynamics in the Fukushima region. Indeed, it is necessary to fully comprehend the

882 frequency and magnitude of heavy rainfall events in the past, in order to properly forecast potential

883 rainfall driven radiocesium export in the future. Installing long-term riverine monitoring stations

884 throughout the fallout impacted catchments to monitor flow and suspended sediment information

885 while providing relationships to radiocesium would provide both a consistent long-term monitoring

886 of radiocesium transfers. This long-term monitoring riverine data should be coupled with long-term

887 monitoring of erosion from soils along with forestry radiocesium transfers to provide a concrete

888 foundation for effective and accurate long-term modelling research through the provision of both

889 reliable long-term calibration data and plot-scale transfer factors necessary to populate catchment

890 scale models.

891 Ultimately, this type of holistic approach, incorporating the different fundamental components

892 driving radiocesium transfer, is necessary. For example, research derived from monitoring at the

893 local forest scale regarding the different transfer dynamics within different tree communities is

894 needed in catchment modelling studies along with erosion data from the hillslope scale runoff

895 research. Indeed a transdisciplinary approach, with a team including hydrologists, geomorphologists,

896 soil and forest scientists, and mathematical modellers, will likely provide the best understanding of

897 radiocesium transfer and migration in the fallout affected region. Through working together, a

898 transdisciplinary team of researchers holds the greatest potential to accurately quantify the transfer

899 of radiocesium from hillslopes to the Pacific Ocean. Indeed, such an approach will also greatly

900 increase our understanding of sediment and material transfers in coastal mountainous environments

901 subject to frequent typhoons.

902 **6. Conclusions**

903 The majority of radiocesium fallout from the FDNPP accident was deposited on forests covering 66%

904 of the region exposed to the highest fallout levels. Although the majority of this fallout was

905 transported to the soil with throughfall, litterfall may become a dominant pathway of contamination

906 transfer in the future. In soils, most of the radiocesium remains in the upper 5 cm of the soil profile

907 except in tilled fields where radiocesium is homogenized throughout the plough layer. Radiocesium is

908 strongly fixed to the finest mineral particles. Runoff generated from snowmelt and heavy rainfall

909 events generates and transfers sediments and their bound radiocesium. In fact, the major typhoons

910 in the region are known to transport the majority of radiocesium from hillslopes to the Pacific Ocean.

911 The FDNPP accident provides an important opportunity to research sediment transfers in general,

912 and radiocesium transfers in particular. Owing to the affinity of radiocesium to fine sediment

913 particles, there is an opportunity to use the accident to understand more about material transfers in

914 coastal mountainous regions subjected to massive typhoons. This understanding may be particularly

915 useful with the anticipated elevated rainfall intensities expected over the next century. Much can be

916 learnt from the Fukushima accident. The application of this learning is fundamental to manage the

917 fallout from this accident now, fallout from potential future accidents, and also simply increase our

918 understanding about the management of contaminants in rivers and riverine geomorphology in

919 general.

920    **Acknowledgements**

924    **References**

925    Achim, P., Monfort, M., Le Petit, G., Gross, P., Douysset, G., Taffary, T., Blanchard, X., Moulin, C.,
926    2014. Analysis of radionuclide releases from the Fukushima Dai-ichi nuclear power plant accident
927    part II. Pure and Applied Geophysics 171, 645-667.
928    Akai, J., Nomura, N., Matsushita, S., Kudo, H., Fukuhara, H., Matsuoka, S., Matsumoto, J., 2013.
929    Mineralogical and geomicrobial examination of soil contamination by radioactive Cs due to 2011
930    Fukushima Daiichi Nuclear Power Plant accident. Physics and Chemistry of the Earth, Parts A/B/C 58,
931    57-67.
932    Akama, A., Kiyono, Y., Kanazashi, T., Shichi, K., 2013. Survey of radioactive contamination of sugi
933    (Cryptomeria japonica D. Don) shoots and male flowers in Fukushima prefecture. Jpn. J. For. Environ
934    55, 105-111.
935    Bu, W., Zheng, J., Aono, T., Tagami, K., Uchida, S., Zhang, J., Honda, M., Guo, Q., Yamada, M., 2013.
936    Vertical distributions of plutonium isotopes in marine sediment cores off the Fukushima coast after
937    the Fukushima Dai-ichi Nuclear Power Plant accident. Biogeosciences 10, 2497-2511.
938    Chartin, C., Evrard, O., Onda, Y., Patin, J., Lefèvre, I., Ottlé, C., Ayrault, S., Lepage, H., Bonté, P., 2013.
939    Tracking the early dispersion of contaminated sediment along rivers draining the Fukushima
940    radioactive pollution plume. Anthropocene 1, 23-34.
941    Chino, M., Nakayama, H., Nagai, H., Terada, H., Katata, G., Yamazawa, H., 2011. Preliminary
942    estimation of release amounts of $^{131}$I and $^{137}$Cs accidentally discharged from the Fukushima Daiichi
943    nuclear power plant into the atmosphere. Journal of nuclear science and technology 48, 1129-1134.
944    Endo, S., Kajimoto, T., Shizuma, K., 2013. Paddy-field contamination with $^{134}$Cs and $^{137}$Cs due to
945    Fukushima Dai-ichi Nuclear Power Plant accident and soil-to-rice transfer coefficients. Journal of
946    environmental radioactivity 116, 59-64.
947    Evrard, O., Chartin, C., Onda, Y., Lepage, H., Cerdan, O., Lefevre, I., Ayrault, S., 2014a. Renewed soil
948    erosion and remobilisation of radioactive sediment in Fukushima coastal rivers after the 2013
949    typhoons. Sci. Rep. 4.
950    Evrard, O., Chartin, C., Onda, Y., Patin, J., Lepage, H., Lefèvre, I., Ayrault, S., Ottlé, C., Bonté, P., 2013.
951    Evolution of radioactive dose rates in fresh sediment deposits along coastal rivers draining
952    Fukushima contamination plume. Scientific reports 3.
953    Evrard, O., Pointurier, F., Onda, Y., Chartin, C., Hubert, A., Lepage, H., Pottin, A.-C., Lefèvre, I., Bonté,
954    P., Laceby, J.P., Ayrault, S., 2014b. Novel Insights into Fukushima Nuclear Accident from Isotopic
955    Evidence of Plutonium Spread along Coastal Rivers. Environ Sci Technol 48, 9334-9340.
956    Evrard, O., Van Beek, P., Gateuille, D., Pont, V., Lefèvre, I., Lansard, B., Bonté, P., 2012. Evidence of
957    the radioactive fallout in France due to the Fukushima nuclear accident. Journal of environmental
958    radioactivity 114, 54-60.
959    Fan, Q., Tanaka, K., Sakaguchi, A., Kondo, H., Watanabe, N., Takahashi, Y., 2014a. Factors controlling
960    radiocesium distribution in river sediments: Field and laboratory studies after the Fukushima Dai-ichi
961    Nuclear Power Plant accident. Applied Geochemistry 48, 93-103.
962    Fan, Q., Yamaguchi, N., Tanaka, M., Tsukada, H., Takahashi, Y., 2014b. Relationship between the
963    adsorption species of cesium and radiocesium interception potential in soils and minerals: an EXAFS
964    study. Journal of Environmental Radioactivity 138, 92-100.
965    Fujii, K., Ikeda, S., Akama, A., Komatsu, M., Takahashi, M., Kaneko, S., 2014. Vertical migration of
966    radiocesium and clay mineral composition in five forest soils contaminated by the Fukushima nuclear
967    accident. Soil Science and Plant Nutrition 60, 751-764.
968    Fujiwara, T., Saito, T., Muroya, Y., Sawahata, H., Yamashita, Y., Nagasaki, S., Okamoto, K., Takahashi,
969    H., Uesaka, M., Katsumura, Y., 2012. Isotopic ratio and vertical distribution of radionuclides in soil
970    affected by the accident of Fukushima Dai-ichi nuclear power plants. Journal of environmental
971    radioactivity 113, 37-44.
972    Gonze, M.-A., Renaud, P., Korsakissok, I., Kato, H., Hinton, T.G., Mourlon, C., Simon-Cornu, M., 2014.
973    Assessment of Dry and Wet Atmospheric Deposits of Radioactive Aerosols: Application to Fukushima
974    Radiocaesium Fallout. Environ Sci Technol 48, 11268-11276.

975 Govers, G., 1985. Selectivity and transport capacity of thin flows in relation to rill erosion. Catena 12,
976 35-49.
977 Groëll, J., Quélo, D., Mathieu, A., 2014. Sensitivity analysis of the modelled deposition of $^{137}$Cs on the
978 Japanese land following the Fukushima accident. International Journal of Environment and Pollution
979 55, 67-75.
980 Hasegawa, M., Ito, M.T., Kaneko, S., Kiyono, Y., Ikeda, S., Makino, S.i., 2013. Radiocesium
981 concentrations in epigeic earthworms at various distances from the Fukushima Nuclear Power Plant
982 6 months after the 2011 accident. Journal of environmental radioactivity 126, 8-13.
983 Hashimoto, S., Ugawa, S., Nanko, K., Shichi, K., 2012. The total amounts of radioactively
984 contaminated materials in forests in Fukushima, Japan. Scientific reports 2.
985 He, Q., Walling, D.E., 1996. Interpreting particle size effects in the adsorption of $^{137}$Cs and
986 unsupported $^{210}$Pb by mineral soils and sediments. Journal of Environmental Radioactivity 30, 117-
987 137.
988 He, Q., Walling, D.E., 1997. The distribution of fallout $^{137}$Cs and $^{210}$Pb in undisturbed and cultivated
989 soils. Applied Radiation and Isotopes 48, 677-690.
990 Hilton, R.G., Galy, A., Hovius, N., Chen, M.-C., Horng, M.-J., Chen, H., 2008. Tropical-cyclone-driven
991 erosion of the terrestrial biosphere from mountains. Nature Geosci 1, 759-762.
992 Iwagami, S., Tsujimura, M., Onda, Y., Nishino, M., Konuma, R., Abe, Y., Hada, M., Pun, I., Sakaguchi,
993 A., Kondo, H., Yamamoto, M., Miyata, Y., Igarashi, Y., Submitted. Temporal changes in dissolved $^{137}$Cs
994 concentrations in groundwater and stream water in Fukushima after the Fukushima Dai-ichi Nuclear
995 power Plant accident.
996 Iwasaki, T., Nabi, M., Shimizu, Y., Kimura, I., 2015. Computational modeling of $^{137}$Cs contaminant
997 transfer associated with sediment transport in Abukuma River. Journal of Environmental
998 Radioactivity 139, 416–426.
999 Jagercikova, M., Cornu, S., Le Bas, C., Evrard, O., 2015. Vertical distributions of $^{137}$Cs in soils: a meta-
1000 analysis. Journal of Soils and Sediments 15, 81-95.
1001 Kakiuchi, H., Akata, N., Hasegawa, H., Ueda, S., Tokonami, S., Yamada, M., Hosoda, M., Sorimachi, A.,
1002 Tazoe, H., Noda, K., 2012. Concentration of 3H in plants around Fukushima Dai-ichi Nuclear Power
1003 Station. Scientific reports 2.
1004 Kanasashi, T., Sugiura, Y., Takenaka, C., Hijii, N., Umemura, M., 2015. Radiocesium distribution in sugi
1005 (Cryptomeria japonica) in Eastern Japan: translocation from needles to pollen. Journal of
1006 environmental radioactivity 139, 398-406.
1007 Kato, H., Onda, Y., Gomi, T., 2012a. Interception of the Fukushima reactor accident-derived $^{137}$Cs,
1008 $^{134}$Cs and $^{131}$I by coniferous forest canopies. Geophys Res Lett 39.
1009 Kato, H., Onda, Y., Teramage, M., 2012b. Depth distribution of 137Cs, 134Cs, and 131I in soil profile
1010 after Fukushima Dai-ichi Nuclear Power Plant Accident. Journal of Environmental Radioactivity 111,
1011 59-64.
1012 Kawamura, H., Kobayashi, T., Furuno, A., In, T., Ishikawa, Y., Nakayama, T., Shima, S., Awaji, T., 2011.
1013 Preliminary numerical experiments on oceanic dispersion of $^{131}$I and $^{137}$Cs discharged into the ocean
1014 because of the Fukushima Daiichi nuclear power plant disaster. Journal of nuclear science and
1015 technology 48, 1349-1356.
1016 Kikawada, Y., Hirose, M., Tsukamoto, A., Nakamachi, K., Oi, T., Honda, T., Takahashi, H., Hirose, K.,
1017 2014. Mobility of radioactive cesium in soil originated from the Fukushima Daiichi nuclear disaster:
1018 application of extraction experiments. J Radioanal Nucl Ch, 1-5.
1019 Kinouchi, T., Yoshimura, K., Omata, T., 2015. Modeling radiocesium transport from a river catchment
1020 based on a physically-based distributed hydrological and sediment erosion model. Journal of
1021 Environmental Radioactivity 139, 407–415.
1022 Kitamura, A., Kurikami, H., Yamaguchi, M., Oda, Y., Saito, T., Kato, T., Niizato, T., Iijima, K., Sato, H.,
1023 Yui, M., 2015. Mathematical modeling of radioactive contaminants in the Fukushima environment.
1024 Nuclear Science and Engineering 179, 105-119.
1025 Kitamura, A., Yamaguchi, M., Kurikami, H., Yui, M., Onishi, Y., 2014. Predicting sediment and cesium-
1026 137 discharge from catchments in eastern Fukushima. Anthropocene 5, 22-31.

Koarashi, J., Atarashi-Andoh, M., Matsunaga, T., Sato, T., Nagao, S., Nagai, H., 2012a. Factors affecting vertical distribution of Fukushima accident-derived radiocesium in soil under different land-use conditions. Science of the Total Environment 431, 392-401.

Koarashi, J., Moriya, K., Atarashi-Andoh, M., Matsunaga, T., Fujita, H., Nagaoka, M., 2012b. Retention of potentially mobile radiocesium in forest surface soils affected by the Fukushima nuclear accident. Scientific reports 2.

Kobayashi, T., Nagai, H., Chino, M., Kawamura, H., 2013. Source term estimation of atmospheric release due to the Fukushima Dai-ichi Nuclear Power Plant accident by atmospheric and oceanic dispersion simulations: Fukushima NPP Accident Related. Journal of Nuclear Science and Technology 50, 255-264.

Koizumi, A., Niisoe, T., Harada, K.H., Fujii, Y., Adachi, A., Hitomi, T., Ishikawa, H., 2013. $^{137}$Cs trapped by biomass within 20 km of the Fukushima Daiichi Nuclear Power Plant. Environ Sci Technol 47, 9612-9618.

Kozai, N., Ohnuki, T., Arisaka, M., Watanabe, M., Sakamoto, F., Yamasaki, S., Jiang, M., 2012. Chemical states of fallout radioactive Cs in the soils deposited at Fukushima Daiichi Nuclear Power Plant accident: Fukushima NPP Accident Related. Journal of nuclear science and technology 49, 473-478.

Kurikami, H., Kitamura, A., Yamaguchi, M., Onishi, Y., 2013. Preliminary Calculation of Sediment and $^{137}$Cs Transport in the Ukedo River of Fukushima. Trans. Am. Nucl. Soc 109, 149-152.

Kurikami, H., Kitamura, A., Yokuda, S.T., Onishi, Y., 2014. Sediment and $^{137}$Cs behaviors in the Ogaki Dam Reservoir during a heavy rainfall event. Journal of Environmental Radioactivity 137, 10-17.

Kuroda, K., Kagawa, A., Tonosaki, M., 2013. Radiocesium concentrations in the bark, sapwood and heartwood of three tree species collected at Fukushima forests half a year after the Fukushima Dai-ichi nuclear accident. Journal of environmental radioactivity 122, 37-42.

Le Petit, G., Douysset, G., Ducros, G., Gross, P., Achim, P., Monfort, M., Raymond, P., Pontillon, Y., Jutier, C., Blanchard, X., 2014. Analysis of radionuclide releases from the Fukushima Dai-Ichi nuclear power plant accident Part I. Pure and Applied Geophysics 171, 629-644.

Lepage, H., Evrard, O., Onda, Y., Chartin, C., Ayrault, S., Bonté, P., 2014a. Tracking the origin and dispersion of contaminated sediments transported by rivers draining the Fukushima radioactive contaminant plume Sediment Dynamics from the Summit to the Sea. IAHS Publ., New Orleans, Louisiana, USA.

Lepage, H., Evrard, O., Onda, Y., Lefèvre, I., Laceby, J.P., Ayrault, S., In Press. Depth distribution of cesium-137 in paddy fields across the Fukushima pollution plume in 2013. Journal of Environmental Radioactivity.

Lepage, H., Evrard, O., Onda, Y., Patin, J., Chartin, C., Lefèvre, I., Bonté, P., Ayrault, S., 2014b. Environmental mobility of $^{110m}$Ag: lessons learnt from Fukushima accident (Japan) and potential use for tracking the dispersion of contamination within coastal catchments. Journal of environmental radioactivity 130, 44-55.

Loffredo, N., Onda, Y., Kawamori, A., Kato, H., 2014. Modeling of leachable $^{137}$Cs in throughfall and stemflow for Japanese forest canopies after Fukushima Daiichi Nuclear Power Plant accident. Science of the Total Environment 493, 701-707.

Long, N.Q., Truong, Y., Hien, P.D., Binh, N.T., Sieu, L., Giap, T., Phan, N., 2012. Atmospheric radionuclides from the Fukushima Dai-ichi nuclear reactor accident observed in Vietnam. Journal of environmental radioactivity 111, 53-58.

Malam Issa, O., Bissonnais, Y.L., Planchon, O., Favis-Mortlock, D., Silvera, N., Wainwright, J., 2006. Soil detachment and transport on field-and laboratory-scale interrill areas: erosion processes and the size-selectivity of eroded sediment. Earth surface processes and landforms 31, 929-939.

Masson, O., Baeza, A., Bieringer, J., Brudecki, K., Bucci, S., Cappai, M., Carvalho, F., Connan, O., Cosma, C., Dalheimer, A., 2011. Tracking of airborne radionuclides from the damaged Fukushima Dai-ichi nuclear reactors by European networks. Environ Sci Technol 45, 7670-7677.

Matsuda, N., Mikami, S., Shimoura, S., Takahashi, J., Nakano, M., Shimada, K., Uno, K., Hagiwara, S., Saito, K., 2015. Depth profiles of radioactive cesium in soil using a scraper plate over a wide area

surrounding the Fukushima Dai-ichi Nuclear Power Plant, Japan. Journal of environmental radioactivity 139, 427-434.

Matsunaga, T., Koarashi, J., Atarashi-Andoh, M., Nagao, S., Sato, T., Nagai, H., 2013. Comparison of the vertical distributions of Fukushima nuclear accident radiocesium in soil before and after the first rainy season, with physicochemical and mineralogical interpretations. Science of the Total Environment 447, 301-314.

Ministry of Education, C., Sports Science and Technology (MEXT), 2012. http://radioactivity.nsr.go.jp/ja/contents/7000/6289/24/203_0928.pdf (2012) (in Japanese).

Minoura, K., Yamada, T., Hirano, S.-i., Sugihara, S., 2014. Movement of radiocaesium fallout released by the 2011 Fukushima nuclear accident. Nat Hazards 73, 1843-1862.

Mishra, S., Arae, H., Sorimachi, A., Hosoda, M., Tokonami, S., Ishikawa, T., Sahoo, S., 2015. Distribution and retention of Cs radioisotopes in soil affected by Fukushima nuclear plant accident. Journal of Soils and Sediments 15, 374-380.

Morgan, R., Quinton, J., Smith, R., Govers, G., Poesen, J., Auerswald, K., Chisci, G., Torri, D., Styczen, M., 1998. The European Soil Erosion Model (EUROSEM): a dynamic approach for predicting sediment transport from fields and small catchments. Earth surface processes and landforms 23, 527-544.

Mori, K., Tada, K., Tawara, Y., Ohno, K., Asami, M., Kosaka, K., Tosaka, H., 2014. An Integrated Watershed Modeling to Assess the Long-term Fate of Fukushima-Derived Radionuclides, in: Ames, D.P., Quinn, N.W.T., Rizzoli, A.E. (Eds.), International Environmental Modelling and Software Society (iEMSs) 7th Intl. Congress on Env. Modelling and Software,, San Diego, CA, USA, .

Motha, J.A., Wallbrink, P.J., Hairsine, P.B., Grayson, R.B., 2002. Tracer properties of eroded sediment and source material. Hydrological Processes 16, 1983-2000.

Mouri, G., Golosov, V., Shiiba, M., Hori, T., 2014. Assessment of the caesium-137 flux adsorbed to suspended sediment in a reservoir in the contaminated Fukushima region in Japan. Environmental Pollution 187, 31-41.

Nagao, S., Kanamori, M., Ochiai, S., Inoue, M., Yamamoto, M., 2014. Migration behavior of [134]Cs and ^{137}Cs in the Niida River water in Fukushima Prefecture, Japan during 2011–2012. J Radioanal Nucl Ch, 1-5.

Nagao, S., Kanamori, M., Ochiai, S., Tomihara, S., Fukushi, K., Yamamoto, M., 2013. Export of [134]Cs and ^{137}Cs in the Fukushima river systems at heavy rains by Typhoon Roke in September 2011. Biogeosciences Discuss. 10, 2767-2790.

Nakanishi, T., Matsunaga, T., Koarashi, J., Atarashi-Andoh, M., 2014. [137]Cs vertical migration in a deciduous forest soil following the Fukushima Dai-ichi Nuclear Power Plant accident. Journal of environmental radioactivity 128, 9-14.

Nakao, A., Ogasawara, S., Sano, O., Ito, T., Yanai, J., 2014. Radiocesium sorption in relation to clay mineralogy of paddy soils in Fukushima, Japan. Science of the Total Environment 468, 523-529.

Nearing, M., Foster, G., Lane, L., Finkner, S., 1989. A process-based soil erosion model for USDA-Water Erosion Prediction Project technology. Trans. ASAE 32, 1587-1593.

Nemoto, K., Abe, J., 2013. Radiocesium absorption by rice in paddy field ecosystems, in: Nakanishi, T., Tanoi, K. (Eds.), Agricultural Implications of the Fukushima Nuclear Accident. Springer, pp. 19-27.

Niimura, N., Kikuchi, K., Tuyen, N.D., Komatsuzaki, M., Motohashi, Y., 2015. Physical properties, structure, and shape of radioactive Cs from the Fukushima Daiichi Nuclear Power Plant accident derived from soil, bamboo and shiitake mushroom measurements. Journal of environmental radioactivity 139, 234-239.

Nishikiori, T., Watanabe, M., Koshikawa, M.K., Takamatsu, T., Ishii, Y., Ito, S., Takenaka, A., Watanabe, K., Hayashi, S., 2015. Uptake and translocation of radiocesium in cedar leaves following the Fukushima nuclear accident. Science of The Total Environment 502, 611-616.

Onishi, Y., Kurikami, H., Yokuda, S., 2014. Simulation of Sediment and Cesium Transport in the Ukedo River and the Ogi Dam Reservoir during a Rainfall Event using the TODAM Code. Pacific Northwest National Laboratory (PNNL), Richland, WA (US).

Phillips, J.M., Russell, M.A., Walling, D.E., 2000. Time-integrated sampling of fluvial suspended sediment: a simple methodology for small catchments. Hydrological Processes 14, 2589-2602.

1131    Pratama, M.A., Yoneda, M., Shimada, Y., Matsui, Y., Yamashiki, Y., 2015. Future projection of
1132    radiocesium flux to the ocean from the largest river impacted by Fukushima Daiichi Nuclear Power
1133    Plant. Scientific reports 5.
1134    Renard, K.G., Foster, G.R., Weesies, G.A., Porter, J.P., 1991. RUSLE: Revised universal soil loss
1135    equation. Journal of soil and Water Conservation 46, 30-33.
1136    Saito, K., Onda, Y., 2015. Outline of the national mapping projects implemented after the Fukushima
1137    accident. Journal of environmental radioactivity 139, 240-249.
1138    Saito, K., Tanihata, I., Fujiwara, M., Saito, T., Shimoura, S., Otsuka, T., Onda, Y., Hoshi, M., Ikeuchi, Y.,
1139    Takahashi, F., 2015. Detailed deposition density maps constructed by large-scale soil sampling for
1140    gamma-ray emitting radioactive nuclides from the Fukushima Dai-ichi Nuclear Power Plant accident.
1141    Journal of environmental radioactivity 139, 308-319.
1142    Saito, T., Makino, H., Tanaka, S., 2014. Geochemical and grain-size distribution of radioactive and
1143    stable cesium in Fukushima soils: implications for their long-term behavior. Journal of environmental
1144    radioactivity 138, 11-18.
1145    Sakaguchi, A., Tanaka, K., Iwatani, H., Chiga, H., Fan, Q., Onda, Y., Takahashi, Y., 2015. Size
1146    distribution studies of $^{137}$Cs in river water in the Abukuma Riverine system following the Fukushima
1147    Dai-ichi Nuclear Power Plant accident. Journal of Environmental Radioactivity 139, 379–389.
1148    Sakai, M., Gomi, T., Nunokawa, M., Wakahara, T., Onda, Y., 2014. Soil removal as a decontamination
1149    practice and radiocesium accumulation in tadpoles in rice paddies at Fukushima. Environmental
1150    Pollution 187, 112-115.
1151    Sansone, U., Belli, M., Voitsekovitch, O.V., Kanivets, V.V., 1996. $^{137}$Cs and $^{90}$Sr in water and suspended
1152    particulate matter of the Dnieper River-Reservoirs System (Ukraine). Science of the Total
1153    Environment 186, 257-271.
1154    Satou, Y., Sueki, K., Sasa, K., Kitagawa, J.-i., Ikarashi, S., Kinoshita, N., 2015. Vertical distribution and
1155    formation analysis of the $^{131}$I, $^{137}$Cs, $^{129m}$Te, and $^{110m}$Ag from the Fukushima Dai-ichi Nuclear Power
1156    Plant in the beach soil. J Radioanal Nucl Ch 303, 1197-1200.
1157    Sawhiney, B., 1972. Selective sorption and fixation of cations by clay minerals: a review. Clays Clay
1158    Miner 20, 93-100.
1159    Schneider, S., Walther, C., Bister, S., Schauer, V., Christl, M., Synal, H.-A., Shozugawa, K., Steinhauser,
1160    G., 2013. Plutonium release from Fukushima Daiichi fosters the need for more detailed
1161    investigations. Scientific reports 3.
1162    Schwantes, J.M., Orton, C.R., Clark, R.A., 2012. Analysis of a nuclear accident: Fission and activation
1163    product releases from the Fukushima Daiichi nuclear facility as remote indicators of source
1164    identification, extent of release, and state of damaged spent nuclear fuel. Environ Sci Technol 46,
1165    8621-8627.
1166    Shimizu, Y., 2003. Mutual relation between riverbed and bank variation characteristics in river
1167    channel landform formation. Annu. J. Hydraul. Eng 47, 643-648.
1168    Shinomiya, Y., Tamai, K., Kobayashi, M., Ohnuki, Y., Shimizu, T., Iida, S.i., Nobuhiro, T., Sawano, S.,
1169    Tsuboyama, Y., Hiruta, T., 2014. Radioactive cesium discharge in stream water from a small
1170    watershed in forested headwaters during a typhoon flood event. Soil Science and Plant Nutrition 60,
1171    765-771.
1172    Shiozawa, S., 2013. Vertical migration of radiocesium fallout in soil in Fukushima, in: Nakanishi, T.,
1173    Tanoi, K. (Eds.), Agricultural implications of the Fukushima nuclear accident. Springer, pp. 49-60.
1174    Shozugawa, K., Nogawa, N., Matsuo, M., 2012. Deposition of fission and activation products after the
1175    Fukushima Dai-ichi nuclear power plant accident. Environmental Pollution 163, 243-247.
1176    Steinhauser, G., 2014. Fukushima's Forgotten Radionuclides: A Review of the Understudied
1177    Radioactive Emissions. Environ Sci Technol 48, 4649-4663.
1178    Tagami, K., Uchida, S., Uchihori, Y., Ishii, N., Kitamura, H., Shirakawa, Y., 2011. Specific activity and
1179    activity ratios of radionuclides in soil collected about 20km from the Fukushima Daiichi Nuclear
1180    Power Plant: Radionuclide release to the south and southwest. Science of the Total Environment 409,
1181    4885-4888.

Takahashi, J., Tamura, K., Suda, T., Matsumura, R., Onda, Y., 2015. Vertical distribution and temporal changes of $^{137}$Cs in soil profiles under various land uses after the Fukushima Dai-ichi Nuclear Power Plant accident. Journal of environmental radioactivity 139, 351-361.

Takeda, A., Tsukada, H., Yamaguchi, N., Takeuchi, M., Sato, M., Nakao, A., Hisamatsu, S.i., 2014. Relationship between the radiocesium interception potential and the transfer of radiocesium from soil to soybean cultivated in 2011 in Fukushima Prefecture, Japan. Journal of environmental radioactivity 137, 119-124.

Tamura, T., 1964. Consequences of activity release: selective sorption reactions of cesium with soil minerals. Nuclear Safety 5, 262–268.

Tanaka, K., Iwatani, H., Sakaguchi, A., Fan, Q., Takahashi, Y., 2015. Size-dependent distribution of radiocesium in riverbed sediments and its relevance to the migration of radiocesium in river systems after the Fukushima Daiichi Nuclear Power Plant accident. Journal of Environmental Radioactivity 139, 390–397.

Tanaka, K., Iwatani, H., Sakaguchi, A., Takahashi, Y., Onda, Y., 2013a. Local distribution of radioactivity in tree leaves contaminated by fallout of the radionuclides emitted from the Fukushima Daiichi Nuclear Power Plant. J Radioanal Nucl Ch 295, 2007-2014.

Tanaka, K., Iwatani, H., Sakaguchi, A., Takahashi, Y., Onda, Y., 2014. Relationship between particle size and radiocesium in fluvial suspended sediment related to the Fukushima Daiichi Nuclear Power Plant accident. J Radioanal Nucl Ch, 1-7.

Tanaka, K., Iwatani, H., Takahashi, Y., Sakaguchi, A., Yoshimura, K., Onda, Y., 2013b. Investigation of Spatial Distribution of Radiocesium in a Paddy Field as a Potential Sink. PLoS ONE 8.

Tanaka, K., Sakaguchi, A., Kanai, Y., Tsuruta, H., Shinohara, A., Takahashi, Y., 2013c. Heterogeneous distribution of radiocesium in aerosols, soil and particulate matters emitted by the Fukushima Daiichi Nuclear Power Plant accident: retention of micro-scale heterogeneity during the migration of radiocesium from the air into ground and river systems. J Radioanal Nucl Ch 295, 1927-1937.

Tazoe, H., Hosoda, M., Sorimachi, A., Nakata, A., Yoshida, M., Tokonami, S., Yamada, M., 2012. Radioactive pollution from Fukushima Daiichi Nuclear Power Plant in the terrestrial environment. Radiation protection dosimetry 152, 198-203.

Teramage, M.T., Onda, Y., Kato, H., Gomi, T., 2014a. The role of litterfall in transferring Fukushima-derived radiocesium to a coniferous forest floor. Science of the Total Environment 490, 435-439.

Teramage, M.T., Onda, Y., Patin, J., Kato, H., Gomi, T., Nam, S., 2014b. Vertical distribution of radiocesium in coniferous forest soil after the Fukushima nuclear power plant accident. Journal of environmental radioactivity 137, 37-45.

Thakur, P., Ballard, S., Nelson, R., 2013. An overview of Fukushima radionuclides measured in the northern hemisphere. Science of The Total Environment 458–460, 577-613.

Torri, D., Sfalanga, M., Del Sette, M., 1987. Splash detachment: runoff depth and soil cohesion. Catena 14, 149-155.

Tsuji, H., Yasutaka, T., Kawabe, Y., Onishi, T., Komai, T., 2014. Distribution of dissolved and particulate radiocesium concentrations along rivers and the relations between radiocesium concentration and deposition after the nuclear power plant accident in Fukushima. Water research 60, 15-27.

Ueda, S., Hasegawa, H., Kakiuchi, H., Akata, N., Ohtsuka, Y., Hisamatsu, S.i., 2013. Fluvial discharges of radiocaesium from watersheds contaminated by the Fukushima Dai-ichi Nuclear Power Plant accident, Japan. Journal of Environmental Radioactivity 118, 96-104.

UNSCEAR, 2000. Sources and effects of ionizing radiation: sources.  United Nations Scientific Committee on the Effects of Atomic Radiation (UNSCEAR). United Nations Publications, New York.

Van Oost, K., Verstraeten, G., Doetterl, S., Notebaert, B., Wiaux, F., Broothaerts, N., Six, J., 2012. Legacy of human-induced C erosion and burial on soil–atmosphere C exchange. Proceedings of the National Academy of Sciences 109, 19492-19497.

Vandaele, K., Poesen, J., Govers, G., van Wesemael, B., 1996. Geomorphic threshold conditions for ephemeral gully incision. Geomorphology 16, 161-173.

Wakahara, T., Onda, Y., Kato, H., Sakaguchi, A., Yoshimura, K., 2014. Radiocesium discharge from paddy fields with different initial scrapings for decontamination after the Fukushima Dai-ichi Nuclear Power Plant accident. Environmental Science: Processes & Impacts 16, 2580-2591.

Wauters, J., Elsen, A., Cremers, A., Konoplev, A., Bulgakov, A., Comans, R., 1996. Prediction of solid/liquid distribution coefficients of radiocaesium in soils and sediments. Part one: a simplified procedure for the solid phase characterisation. Applied Geochemistry 11, 589-594.

Wetherbee, G.A., Gay, D.A., Debey, T.M., Lehmann, C.M., Nilles, M.A., 2012. Wet deposition of fission-product isotopes to North America from the Fukushima Dai-ichi Incident, March 2011. Environ Sci Technol 46, 2574-2582.

Wischmeier, W.H., Smith, D.D., 1958. Rainfall energy and its relationship to soil loss. Transactions American Geophysical Union 39, 285-291.

Yamada, S., Kitamura, A., Kurikami, H., Yamaguchi, M., Malins, A., Machida, M., 2015. Sediment and $^{137}$Cs transport and accumulation in the Ogaki Dam of eastern Fukushima. Environmental Research Letters 10, 014013.

Yamaguchi, M., Kitamura, A., Oda, Y., Onishi, Y., 2014. Predicting the long-term $^{137}$Cs distribution in Fukushima after the Fukushima Dai-ichi nuclear power plant accident: a parameter sensitivity analysis. Journal of Environmental Radioactivity 135, 135-146.

Yamaguchi, N., Eguchi, S., Fujiwara, H., Hayashi, K., Tsukada, H., 2012. Radiocesium and radioiodine in soil particles agitated by agricultural practices: Field observation after the Fukushima nuclear accident. Science of The Total Environment 425, 128-134.

Yamashiki, Y., Onda, Y., Smith, H.G., Blake, W.H., Wakahara, T., Igarashi, Y., Matsuura, Y., Yoshimura, K., 2014. Initial flux of sediment-associated radiocesium to the ocean from the largest river impacted by Fukushima Daiichi Nuclear Power Plant. Scientific Reports 4.

Yoshida, N., Kanda, J., 2012. Tracking the Fukushima radionuclides. Science 336, 1115-1116.

Yoshida, N., Takahashi, Y., 2012. Land-surface contamination by radionuclides from the Fukushima Daiichi Nuclear Power Plant accident. Elements 8, 201-206.

Yoshihara, T., Hashida, S.-n., Abe, K., Ajito, H., 2014a. A time dependent behavior of radiocesium from the Fukushima-fallout in litterfalls of Japanese flowering cherry trees. Journal of environmental radioactivity 127, 34-39.

Yoshihara, T., Matsumura, H., Hashida, S.-n., Nagaoka, T., 2013. Radiocesium contaminations of 20 wood species and the corresponding gamma-ray dose rates around the canopies at 5 months after the Fukushima nuclear power plant accident. Journal of environmental radioactivity 115, 60-68.

Yoshihara, T., Matsumura, H., Tsuzaki, M., Wakamatsu, T., Kobayashi, T., Hashida, S.-n., Nagaoka, T., Goto, F., 2014b. Changes in radiocesium contamination from Fukushima in foliar parts of 10 common tree species in Japan between 2011 and 2013. Journal of environmental radioactivity 138, 220-226.

Yoshikawa, N., Obara, H., Ogasa, M., Miyazu, S., Harada, N., Nonaka, M., 2014. $^{137}$Cs in irrigation water and its effect on paddy fields in Japan after the Fukushima nuclear accident. Science of The Total Environment 481, 252-259.

Yoshimura, K., Onda, Y., Kato, H., 2015a. Evaluation of radiocaesium wash-off by soil erosion from various land uses using USLE plots. Journal of Environmental Radioactivity 139, 362–369.

Yoshimura, K., Onda, Y., Sakaguchi, A., Yamamoto, M., Matsuura, Y., 2015b. An extensive study of the concentrations of particulate/dissolved radiocaesium derived from the Fukushima Dai-ichi Nuclear Power Plant accident in various river systems and their relationship with catchment inventory. Journal of Environmental Radioactivity 139, 370–378.